Structural Geology - Tectonics - Geomechanics

RWTH AACHEN UNIVERSITY

Report to Nedmag BV.

Billitonweg 1 - 9640 AE Veendam - The Netherlands

Nedmag Winningsplan 2018

Squeeze mining-induced stress changes in the faulted overburden of the Veendam salt Pillow

Janos L. Urai

Structural Geology, Tectonics and Geomechanics

RWTH Aachen University, Lochnerstrasse 4-20

D-52056 Aachen, Germany

e-mail: j.urai@ged.rwth-aachen.de

www.ged.rwth-aachen.de

Alexander F. Raith

DEEP.KBB GmbH

https://deep-kbb.de

Eyhauser Allee 2a, 26160

Bad Zwischenahn, Germany

Aachen, 10.11.2018

Summary

The aim of this project was to study the stress development in the faulted overburden of the Veendam Salt pillow caused by squeeze mining in a set of new caverns (VE-5, -6, -7 and -8), in addition to the stress changes caused by Nedmag's existing caverns, and to investigate if faults in the overburden of the Veendam Salt pillow could be reactivated by this. We consider the evolution during 65 years in two situations: (i) reactivation by salt solution mining induced stress changes with an intact rock salt roof and hydrostatic pore pressure in the overburden, and (ii) reactivation by pore pressure increases in the overburden in case of a fractured halite roof and intrusion of high pressure brine into the overburden (the event of 20 April 2018, with rapid pressure loss in Nedmag's VE - TR cavern cluster and the inferred formation of a large vertical fluid driven fracture in the overburden).

In the case of an intact rock salt roof:

Here we follow up on an earlier study (Raith and Urai 2017) which investigated possible fault reactivation by Nedmag's squeeze solution mining induced stress changes above the present caverns, using geomechanical modelling and 3D seismic mapping of the overburden faults. This study demonstrated that in most of the overburden, Nedmag's current salt solution mining reduces the shear stress to mechanically more stable conditions, in agreement with theory and earlier simulations. In a limited volume of the overburden, shear stresses increase, but this increase is small and the stress path is likely to be far from the failure criterion for fault reactivation. Therefore, reactivation of the existing, tectonically inactive faults in the overburden due to these stress changes was interpreted to be very unlikely.

The present study builds on these results and uses similar Finite Element geomechanical models to study the additional stress changes caused by squeeze mining in a second cavern field (VE-5, -6, -7 and -8) in a set of models of this configuration, to a maximum subsidence of 95 cm at the deepest point of the composite subsidence bowl. The study was carried out in three steps:

First, a model of the initial (before mining) stress state in the tectonically inactive Veendam salt pillow and its overburden was investigated. A plane strain model was built based on a 3D seismic profile, using similar mechanical properties as in the earlier study, and let to evolve for 10 million years to a geologically stable state, with the buoyancy of the Veendam salt pillow compensated by the stress field of the overburden. Because horizontal stresses in the rocks above the salts in the Northern Netherlands are poorly known, this way a more appropriate initial stress state model is obtained than used in previous models.

Second, a set of models with the same stratigraphy and properties (but with horizontal layers) was used to explore the difference between the stress field caused by squeeze mining in a plane strain model and an axisymmetric model. These are both techniques commonly used to model overburden deformation above salt caverns.

Results of these models show that plane strain models are conservative in all cases: if a plane strain model does not lead to fault reactivation, then its axisymmetric equivalent is less likely to do so. Therefore, the plain strain model was selected for further calculations.

Third, we superpose squeeze mining of the existing cavern field on our plane strain initial stress model, starting from the initial geologically stable situation to the present day. Results were in qualitative agreement with the outcome of the earlier study of this phase. Then we superposed on this situation a second phase of squeeze mining in the present caverns and in a second cavern field (VE-5, -6, -7 and -8). The stress field caused by this second cavern field is similar in shape but smaller

in magnitude to what has been computed above the existing caverns. These models reproduce the prognosed subsidence profile. We evaluated our results by computing the proximity to failure in the overburden: a measure of how far the stress is from reactivating an optimally oriented cohesionless fault.

Results show that even for models that are conservative, the proximity to failure (shear stress divided by maximum shear stress to get plasticity) remains below unity (100%) everywhere in the overburden. Therefore, if the halite roof is intact, reactivation of existing, tectonically inactive faults in the overburden due to stress changes caused by squeeze mining is interpreted to be very unlikely.

Interaction with stresses caused by gas production ("gestapelde mijnbouw") is difficult to fully assess without knowing the stresses caused by gas production in the nearby Groningen and Annerveen fields. Subsidence caused by the two mining activities is clearly superposed, and so are stress changes in the subsurface. However, for the gas production, the large stress changes and fault reactivations occur in the reservoir below the Zechstein salt. Until today there is no measurable effect of these interactions besides the combined subsidence in the Veendam area. Although we are not in the position to quantify the overburden stress changes caused by gas production – this is the expertise of NAM- but in our opinion this is significantly smaller than that caused by solution mining. Therefore, our conclusions are likely not affected by the presence of nearby gas production below the Zechstein salt.

In the case of a fractured Halite roof:

Here we consider the recent event of 20 April 2018, with rapid pressure loss in Nedmag's TR cavern cluster and the inferred formation of a vertical fluid driven fracture in the overburden. The event itself coincides in time to a small seismic event as detected by seismometers. Within the context of this study, the question is if such an event could lead to fault reactivation. *If* the normal faults in the overburden above the leak point were permeable enough to be penetrated by the fluid, simple mechanical considerations show that the fluid pressures in the fracture (these are slightly higher than the minimum total stress in the surrounding rocks) were potentially high enough to induce reactivation of some existing faults in the overburden, directly during the fracture's propagation or during the slower pore pressure penetration from the fracture walls into larger rock volumes. However, the absence of a larger seismic event during and after the formation of the event of 20 April 2018 is consistent with the inference that the faults are *not permeable* enough to be significantly penetrated by the fluid, as they predominantly contain low permeability clay-rich gouge and tectonic veins (as indicated by the clay-rich stratigraphy and as shown by field studies of analogues, and by the absence of indicators for open fractures in offset wells).

These fault structures in the faulted overburden can be safely assumed to be similar over the whole Veendam pillow. Therefore, if in the future a leak of the rock salt roof would occur, we estimate the risk of a larger seismic event as low.

Introduction

The aim of this project was to study the stress development in the faulted overburden of the Veendam Salt pillow caused by squeeze mining in a set of new caverns (VE-5, -6, -7 and -8), in addition to the stress changes caused by Nedmag's existing caverns, and to investigate if faults in the overburden of the Veendam Salt pillow could be reactivated by this. We consider the evolution during 65 years in two situations: reactivation by salt solution mining induced stress changes with an intact rock salt roof and hydrostatic pore pressure in the overburden and reactivation by pore pressure increases in the case of a failed halite roof and intrusion of high-pressure brine into the overburden.

Part 1: the case of an intact Rock Salt roof

Method

The general approach used in this study is similar to that of earlier studies such as Fokker et al., (1995) and the same as in our previous report (Raith and Urai 2017). To simulate the stress changes in the Veendam Salt Pillow and its overburden, caused by squeeze mining of a cavern field, the Finite Element Method (FEM) software 3DS Abaqus was used. Abaqus is widely used for engineering and material science applications and sets a benchmarked industry standard (http://www.3ds.com/).

Results were evaluated considering a cohesionless Mohr-Coulomb criterion for the brittle overburden. This criterion is very conservative for consideration of fault reactivation. If this criterion is reached in a given volume of cohesive rock, there has to be an optimally oriented, cohesionless pre-existing fault in this place for reactivation of this fault. This allowed us to keep the properties of the overburden elastic, because no plasticity calculations were required.

The models were calculated in steps. In the first stage a geostatic stress is established which is followed by a second step to let the model equilibrate in geologic time. In the third phase the pressure in the cavern field is lowered to produce about 65 cm of subsidence in the center of the subsidence bowl. Then we superposed a second phase of squeeze mining on this situation in the present caverns and in a second cavern field (VE-5, -6, -7 and -8). We evaluated the stress development caused by squeeze mining during these two steps.

FE model setup

The Veendam Pillow has an elliptical shape striking NE-SW and a diameter of about 10 km (Fig. 1). It is surrounded by salt withdrawal basins and other salt structures (i.e. pillows or diapirs) further away (Strozyk et al., 2014). The Veendam and Tripscompagnie cavern field is located around the crest of the eastern part of the pillow. The 13 existing wells are distributed in an area with a diameter of 2.5 km inside the Zechstein-III 1b to 3b K-Mg salt layers, with a highly irregular, partly connected solution mined cavern system. The geologic evolution and structure of the Veendam Pillow is described in detail in recent publications (Raith et al., 2016. Raith et al., 2017, Raith 2017).

In our first report, we studied models with radial symmetry, to estimate the stress above one cavern cluster. Here we consider two cavern clusters and this is not well studied in radial symmetric models. If accurate data about mechanical properties, initial stresses and cavern geometries were available, one could consider full 3D models (van der Zee et al.,

2011). However, in our case the available accuracies do not justify this effort, and we chose a combination of 2D plane strain and axisymmetric models to approach this case with the addition of a new set of caverns.

First, we further developed the models of the initial (before the beginning of mining) stress state in the tectonically inactive Veendam salt pillow and its overburden (Fig. 1). This model contains the geometries of both the existing and the future cavern clusters but these are not active at this stage. The new plane strain model was built with a geometry based on a 3D seismic profile, using similar mechanical properties as in the first report, and let to evolve for 10 million years, after which time the model was stable, with the buoyancy of the Veendam salt pillow compensated by the stress field of the overburden, and with horizontal stresses in the expected range. Because horizontal stresses in the subsurface (above the salt) of the Northern Netherlands are poorly known, a more appropriate initial stress state is difficult to achieve at present.

Second, we used a set of plane strain and axisymmetric models (Figs. 10 - 19) with the same stratigraphy but with horizontal layers to explore the difference between the stress fields caused by squeeze mining in plane strain and axisymmetric models. We built a set of models with one central cavern (Fig. 10) and models with a number of distributed caverns (Fig. 15). The caverns are located in the K-Mg salt layer which is much softer than the surrounding rock salt.

After this, we superposed squeeze mining of the first (existing) cavern field on our plane strain model which is based on the 3D seismic profile, starting from the initial geologically stable situation. Results agreed with our first study, as expected. Finally, we superposed on this situation a second phase of squeeze mining in a second cavern field (Figs 2 – 9).

The models were meshed using either 8-node biquadratic plane strain quadrilateral (CPE8) or 8-node biquadratic axisymmetric quadrilateral (CAX8) elements.

Boundary conditions were as follows: (1) bottom of the model fixed in Depth (Y) direction; (2) both sides fixed in horizontal (X) direction; (3) cavern walls fixed in step 1 and 2, pressure boundary in step 3; (4) gravity active in the whole model; (5) The starting value of minimum horizontal to vertical total stress ratio (K_h) was calculated from gravity and density assuming 0.8 as target value in the overburden and 1.0 in the salt. This is then equilibrated into the initial heterogeneous stress situation over geologic time.

Layers

To simulate the mechanical response of the overburden to cavern convergence, the model was subdivided into several units with different rheology and mechanical properties (Fokker, 1995; Fokker and Visser, 2014) (Fig. 1, Table 1). The Rotliegend subsalt layer is overlain by Zechstein salt. Inside the Zechstein halite unit, the discontinuous anhydrite stringers and one K-Mg salt layer are present to represent the softer ZIII 1b to 3b layers. The suprasalt sediments are simplified to a Triassic unit overlain by the Lower and Upper Cretaceous and the Tertiary - Quaternary sediments of the Upper North Sea Supergroup. These units are thicker in the basins than above the pillow center.

While the rheology of the salt includes elastic and power law creep behavior (Table 1), the overburden is modeled as elastic: since the aim of this study is to clarify if the overburden stresses during elastic deformation can reach the Mohr Coulomb plasticity criterion, there is no need to include plasticity in the overburden.

Salt rheology

Under the conditions of squeeze mining, evaporites deform elastically and by creep, without dilatancy (Urai et al., 2008). The plastic deformation of evaporites is described by some combination of (power law) dislocation creep and (linear) fluid assisted pressure solution / precipitation creep. Since squeeze mining leads to a geologically rapid deformation, we decided

to use power law creep only (Urai et al., 2008). We infer that including the weaker PS creep, while possible, will not significantly change the results relevant to this report.

The rheology of the mixed potassium and magnesium (K-Mg) salts in the 1b layer was chosen to have the same stress exponent as rock salt, but much weaker than rock salt, to simulate a package of Carnallite, Halite and Bischofite (Table 1, Raith, 2017). Again, this is a simplification, but considering that the stress changes in the overburden occur at a distance from the 1b layer which is more than 10x the thickness of typical Bischofite layers, we infer that this will not significantly change the results relevant to this report. Note that as an improvement to our previous models, we have now used more realistic, weaker K-Mg salt rheology than in the previous study (creep multiplier = 1e-39).

Table 1:

Name	Depth in pillow center [m]	Depth in the basins [m]	Density [Kg/m³]	Young's Modulus [GPa]	Poisson´s Ratio	Creep Multiplier	Creep Exponent
Quat. + Tertiary	0 - 400	0 - 800	2000	1	0.38	-	-
U. Cretaceous	400 - 900	800 - 1400	2300	10	0.18	-	-
L. Cretaceous	900 - 1000	1400 - 1500	2350	15	0.23	-	-
Triassic	1000 - 1400	1500 - 2100	2450	10	0.25	-	-
Rock Salt	1400 to 3300	2100 - 3300	2040	30	0.25	1e-44	5
K-Mg salt	1560 - 1630	2230 - 2260	2040	30	0.25	1e-39	5
Anhydrite	stringers	stringers	2600	30	0.25	1e-54	5
Rotliegend	3300 - 5000	3300 - 5000	2600	15	0.18	-	-

Model Results

Initial stress

Stresses in the models were computed as total stresses, assuming drained behavior and hydrostatic pore pressure everywhere with SG = 1.0. For stability analyses, effective stresses were computed, using hydrostatic pore pressure. Figures 2, 3, 4, (top pictures) shows the evolution of stress using contours of the minimum and maximum principal stresses and the shear stresses. Note that the stress contours in the starting model are not horizontal as commonly assumed, due to the stress redistribution required for a geologically stable situation above the Veendam pillow.

We note that in general the present day in-situ stress state in the Northern Netherlands is not well known because there are very few measurements. This causes a significant uncertainty in subsurface integrity analyses which compute the changes in stress, starting from the initial stress. In this study, in contrast to other studies, we aimed to establish an initial stress state which is geologically stable, as a first step towards addressing this issue.

We do note that the most likely orientation of the initial minimum principal stress (the minimum horizontal stress) in this part of the Netherlands is NE-SW (Gent et al., 2009). This orientation is not consistent with movement of the existing faults in the overburden of the Veendam pillow, suggesting that the initial stress is not optimal for fault reactivation, and also in agreement with the conclusion from recent studies that the initial stress state in the subsurface of the Groningen Field was not critically stressed. We will return to this point later in the report.

Subsidence

The subsidence bowl geometry (Fig 5) resembles the results by Fokker and Visser (2014). The displacement is dominantly vertical. In the layers above the Triassic, the zone of vertical motion gets wider, as expected and therefore a horizontal component of movement towards the center of the cavern field is also significant. Inside the Triassic, minor local horizontal stretching in the areas between the caverns is computed. Note also that vertical displacement at top salt level is higher than at surface, causing vertical strain in the overburden. Subsidence in the horizontally layered models is shown in Figs. 13 and 18. Note that these models, for computational reasons, were not all done to a surface subsidence of 65 cm, but since the overburden is elastic and these models were made to compare axisymmetric models with plane strain ones, the conclusion of the comparison is the same for different values of maximum subsidence.

Stress development

Models with horizontal layers

In both the single cavern and multiple cavern models, the stress patterns in the overburden are similar, for the axisymmetric and the plane strain models. Results are shown in a series of comparison diagrams in Figs. 10 - 19. One can distinguish two zones, which were also discussed in detail in the previous report. Zone I is located directly above the caverns, while zone II is at 300 to 1000 m distance from the caverns.

Zone I: This zone is characterized by a lowering of differential stress. In the Triassic, above the caverns the decrease of differential stress (σ_1 - σ_3) is mostly caused by a reduction of the sub vertical σ_1 principal stress (Fig. 11). The sub-horizontal σ_3 is also lowered in this area with smallest values in the area between caverns. Inside the Cretaceous, lower differential stress is mainly caused by an increase of the horizontal σ_3.

Zone II: In this zone increased differential stress values of up to 1 MPa can be observed. The increase is caused by a rise of vertical σ_1 stress in that area.

Results of these models clearly show that plane strain models are conservative in all cases: if a plane strain model does not lead to fault reactivation, then its axisymmetric equivalent will also not lead to fault reactivation.

Plane strain models based on seismic profile

Based on these results, we inferred that the plane strain models of Fig. 1 provide a reasonable and conservative basis to evaluate stresses above the two cavern fields. First we superposed squeeze mining of the existing cavern field on our plane strain initial stress model, starting from the initial geologically stable situation to the present day ("after 50 a" in Fig. 2 – 9) . Results are in agreement with the outcome of the earlier study and with the observed subsidence. Then we superposed on this situation a second phase of squeeze mining in the present caverns and in a second cavern field (VE-5, -6, -7 and -8). The stress field caused by this second cavern field is similar in shape but smaller in magnitude to what has been computed

above the existing caverns. These models reproduce the prognosed subsidence profile. We evaluated our results by computing the proximity to failure in the overburden: a measure of how far the stress is from reactivating an optimally oriented cohesionless fault. This is illustrated in a Mohr diagram in Fig. 7 and 8.

Results show, as expected, that the shear stress in the overburden is reduced directly above the caverns and increases slightly to the East of the Ve- Tr cavern field. We also note that the Von Mises shear stress increases in the Halite roof of the caverns, and also in the stringers below the caverns (Fig. 7 and 8). The proximity of failure decreases to more stable configurations above the caverns, and increases slightly in some areas, but it does not come close to the (already conservative) failure envelope anywhere in the overburden.

Faults in the overburden

As part of a study of the risk of fault reactivation in the overburden of the Veendam Pillow, the faults in the overburden were mapped. Results of this were shown in the previous report and are reproduced here in Figure 20. While the quality of the 3D seismic is reasonable, only the general pattern of the faults could be mapped, keeping in mind the well-known problems and limitations of fault interpretations. In the overburden of the Veendam Pillow two dominant fault directions are present: NE-SW striking normal faults parallel to the crest and N-S striking normal faults in NE and SW of the Veendam Pillow (Fig. 20). None of the faults can be shown to continue to the surface, in agreement with the absence of neo-tectonic activity in the area, and none of these faults are optimally oriented for reactivation in the present-day stress field with the maximum horizontal stress oriented NW-SE.

Discussion

The models presented here reproduce the observed and prognosed subsidence (Fig. 21) but are only a subset of many different models (with different cavern sizes, pressure histories, mechanical properties, etc.) which can be used to match the observed subsidence and production over time by choosing from a range of mechanical properties and loading histories. In our models, no history match with pressure data and squeeze volumes was attempted. In comparison with the models of Fokker et al., 1995, and Raith 2017 we have used a more complicated cavern model, and attempted to compute a more realistic initial stress distribution in the Veendam Pillow. The initial stresses are stable over geologic time, without plasticity in the overburden, consistent with the absence of neo-tectonics and consistent with the scarce data on LOT results in the Bunter shown in Fig. 22. We infer, because the models match the subsidence and because the overburden is elastic, that different realizations of this model would produce similar overburden stress changes.

Considering the deformations in the overburden, it can be seen that the presence of a series of caverns cause interacting stress fields in the overburden, (Fig. 4, Fig. 9). In the shallower Cretaceous lower differential stresses are primarily caused by horizontal shortening and therefore higher horizontal stresses. Small increases in differential stress can only be observed above edges of the caverns. Here horizontal stretching due to salt flow towards the caverns decreases the horizontal stress.

Noting that plain strain models and cohesionless MC criterion are conservative, (assuming that optimally oriented faults are present everywhere), we evaluated the stress changes in the overburden, results are shown in (Figs. 7, 8 and 9). In part of the overburden, squeeze mining makes the stress in the overburden more stable, in other areas the proximity to failure becomes slightly higher but still far from 100%.

Interaction with stresses caused by Gas production: (gestapelde mijnbouw)

Interaction with stresses caused by Gas production is difficult to fully assess without knowing the stresses caused by gas production in the nearby Groningen and Annerveen fields. Subsidence caused by the two mining activities is clearly superposed, and so are stress changes in the subsurface. However, for the gas production, the large stress changes and fault reactivations occur in the reservoir below the Zechstein salt. These gas-reservoir level stress changes are probably less intense in the Veendam area than in the center of the Groningen Gas Field because the Veendam caverns are located in between the Groningen and Annerveen fields and published maps show no significant gas accumulation below the Veendam caverns. Stress in the suprasalt rocks is expected to change much less due to gas production, and also more gradually because of the absence of local pore pressure changes and because of decoupling by salt, but these effects have not been quantified. It is possible that (because the Veendam Pillow is above a graben or depression between the gas reservoirs of the Groningen field and the Annerveen field with their associated subsidence bowls), there is a possible "edge" effect of gas production-induced increase of shear stress in the overburden of the Groningen field which may interact with the squeeze mining-induced stresses in the overburden. On the other hand, very small squeeze mining-induced stress changes (<0.5 MPa) are also induced in the (1000 m deeper) Rotliegend reservoir despite the decoupling by the Zechstein salt, but our models have not been calibrated to give accurate estimates of this.

Until today there is no measurable effect of these interactions besides the combined subsidence in the Veendam area. Although we are not in the position to quantify the overburden stress changes caused by gas production – this is the expertise of NAM - in our opinion this is significantly smaller than that caused by solution mining. Therefore, our conclusions are likely not affected by the presence of nearby gas production below the Zechstein salt.

Conclusion

Results of these models show that even for models that are conservative, the proximity to failure remains below unity (100%) everywhere in the overburden. Therefore, if the halite roof is intact, reactivation of existing, tectonically inactive faults in the overburden due to stress changes caused by squeeze mining is interpreted to be very unlikely.

Part 2: the case of a failed rock salt roof

Here we consider the recent leakage event of 20 April 2018, with rapid pressure loss in Nedmag's TR cavern cluster and the inferred formation of a large vertical fluid driven fracture in the overburden (Van den Hoek, 2018). The event coincides in time to a small seismic event of less than M_w=0.5 in the vicinity of the brine field which could have been associated with the propagating fracture. Within the context of this study, the question is if such an event could lead to fault reactivation in the overburden. Because the fluid pressures in the overburden can in this case become much higher than hydrostatic (up to the minimum rock stress) and because rock failure is controlled by effective stress, this case is different than the one considered in Part 1.

We recall the general trend of cavern operating pressures and stresses in the Zechstein and in the overburden, and compare this with the data shown in Fig. 3 which is a contour plot of the minimum principal stress in the model. In Fig. 23 we show a contour plot of the change in minimum principal stress between the initial and the final ("65 a") stage. This shows that above the caverns the minimum stress in the Halite roof is locally reduced by about 4 MPa, the initial difference between cavern pressure and minimum stress in the Halite roof (Fig. 22). The pressure in the caverns in this case is thus

comparable to the minimum principal stress in the halite roof. The directions of the minimum principal stress in the Halite roof above the caverns vary substantially (Fig. 9) and the Von Mises stress in the Halite roof is increased to a few MPa, leading to some salt flow. Thus, our models also reproduce the conditions for flow of cavern fluid through the halite roof. A more detailed analysis of this is provided in a separate report by (Fokker in prep, this Winningsplan).

The cavern fluid which enters the overburden has thus a higher pressure than the minimum principal stress in the overburden and creates a sub vertical fracture. The path of this fracture could cross existing fault zones, and as shown by Van den Hoek (2018), the high pore pressure in the fracture can penetrate into the wall of the fracture over several 100 m, strongly raising the pore pressure in a substantial volume. The effect of this on the normal faults in the overburden above the leak point which are permeable enough to be penetrated by the fluid is shown by a 3D Mohr diagram of Fig. 24 and 25. These simple mechanical considerations show that the fluid pressures in the fracture (which are slightly higher than the minimum total stress in the surrounding rocks) are potentially high enough to induce reactivation of many but not all orientations of existing faults in the overburden, directly during the fracture's propagation or during the slower pore pressure penetration from the fracture walls into larger rock volumes. However, the absence of a larger seismic event during and after the formation of the event of 20 April 2018 is consistent with the inference that the faults are *not permeable* enough to be penetrated by the fluid over significant areas, as they predominantly contain low permeability clay-rich gouge and tectonic veins. This is indicated by the clay-rich stratigraphy and is shown by field studies of analogues, and by the absence of indicators for open fractures in offset wells. Alternatively, some faults in the overburden could have moved by non-seismic slip during the event of 20 April 2018. The structures in the faulted overburden can be assumed to be similar over the whole Veendam pillow, and the experience with the event of 20 April 2018 suggests that although this event could have led to fault reactivation, there was no seismic event either because faults were not reactivated or because slip was aseismic. We can use this reasoning to conclude that if in the future another leak of the rock salt roof would occur, the effect on faults would be similar, and we estimate the risk of a larger seismic event in this case as low.

References

Fokker, P.A., 1995. The behaviour of salt and salt caverns. Dissertation, Delft University of Technology.

Fokker, P.A., Visser, J., 2014. Estimating the distribution of salt cavern squeeze using subsidence measurements, in: 48 Th US Rock Mechanics / Geomechanics Symposium. American Rock Mechanics Association, Minneapolis, p. ARMA 14 – 7357.

Fokker, P.A., Urai, J.L. and Steeneken, P.V. (1995). Production-induced convergence of solution mined caverens in magnesium salts and associated subsidence. In: Barends, Brouwer and Schröder (eds): Land subsidence. Natural causes, measuring techniques, the Groningen gas field. Proceedings of the fifth international conference on land subsidence, Den Haag, the Netherlands, 16-20 Oct. 1995, p. 281-289.

Raith, AF F Strozyk, J Visser, JL Urai (2016) Evolution of rheologically heterogeneous salt structures: a case study from the NE Netherlands. Solid Earth 7 (1), 67

Raith, A.F. 2017 Internal deformation of salt bodies with large mechanical contrast: a case study of the Veendam salt Pillow, the Netherlands PhD Thesis, RWTH Aachen University, DOI: 10.18154/RWTH-2018-223888

Raith, AF JL Urai, J Visser (2017) Structural and microstructural analysis of K–Mg salt layers in the Zechstein 3 of the Veendam Pillow, NE Netherlands: development of a tectonic mélange during salt flow. Netherlands Journal of Geosciences 96 (4), 331-351

Raith Alexander F. and Janos L. Urai (2017) Squeeze mining- induced stress changes in the faulted overburden of the Veendam salt Pillow. Report to Nedmag Industries Mining & Manufacturing B.V., and in press, SaltMech IX conference.

Schléder, Z., Urai, J.L., 2005. Microstructural evolution of deformation-modified primary halite from the Middle Triassic Röt Formation at Hengelo, The Netherlands. Int. J. Earth Sci. 94, 941–955. doi:10.1007/s00531-005-0503-2

Urai, J.L., 1983. Water assisted dynamic recrystallization and weakening in polycrystalline Bischofite. Tectonophysics 96, 125–157. doi:10.1016/0040-1951(83)90247-0

Urai, J.L., Schléder, Z., Spiers, C.J., Kukla, P.A., 2008. Flow and Transport Properties of Salt Rocks, in: Dynamics of Complex Intracontinental Basins: The Central European Basin System. pp. 277–290. doi:978-3-540-85085-4

van Eekelen, H.A., Urai, J.L., Hulsebos, T., 1981. Creep of Bischofite, in: Proceedings, 1st Conference on the Mechanical Behaviour of Salt. Pennsylvania.

van Gent, H., Back, S., Urai, J., Kukla, P. and Reicherter, K. (2009). Paleostresses of the Groningen area, the Netherlands: Results of a seismic based structural reconstruction. Tectonophysics 470(1-2): 147-161.

van der Zee Wouter, Cem Ozan, Martin Brudy, Marc Holland (2011) 3D Geomechanical Modeling of Complex Salt Structures. 2011 Pepr presented at: SIMULIA Customer Conference

Strozyk, F., Urai, J.L., van Gent, H.W., de Keijzer, M., Kukla, P.A., 2014. Regional variations in the structure of the Permian Zechstein 3 intrasalt stringer in the northern Netherlands: 3D seismic interpretation and implications for salt tectonic evolution. Interpretation 2, SM101-SM117.

Van den Hoek, P, 2018, Analysis of TR-2 salt cavern leakage incident of 20 April 2018 PanTerra Report for Nedmag.

FIGURES

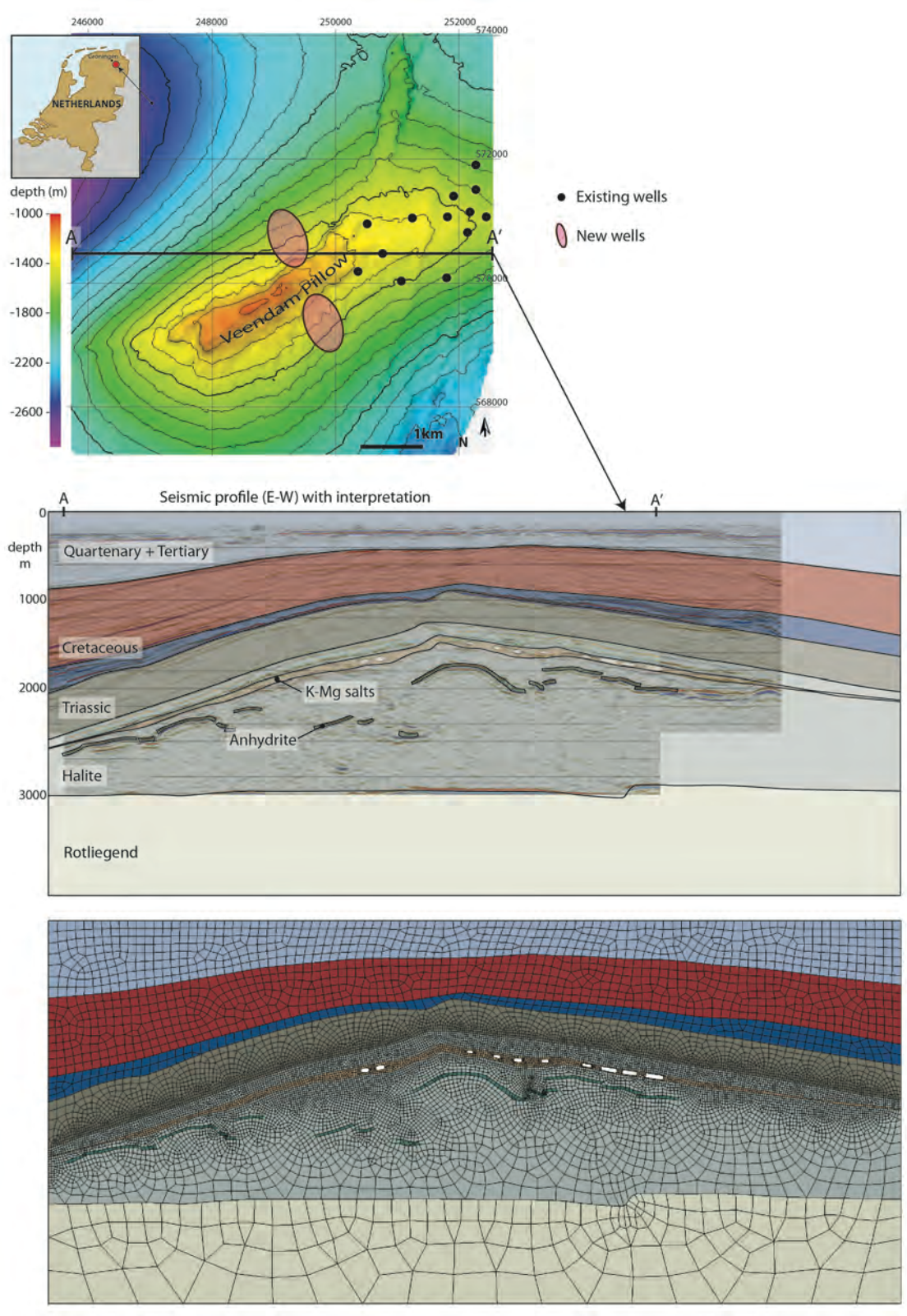

Fig. 1 - 3D seismic-based map showing the depth of the ZE III 1b layer and the existing and new well locations. Interpreted seismic profile along the line indicated, showing the different units defined in the geomechanical modelling, and the Finite Element mesh constructed based on this profile.

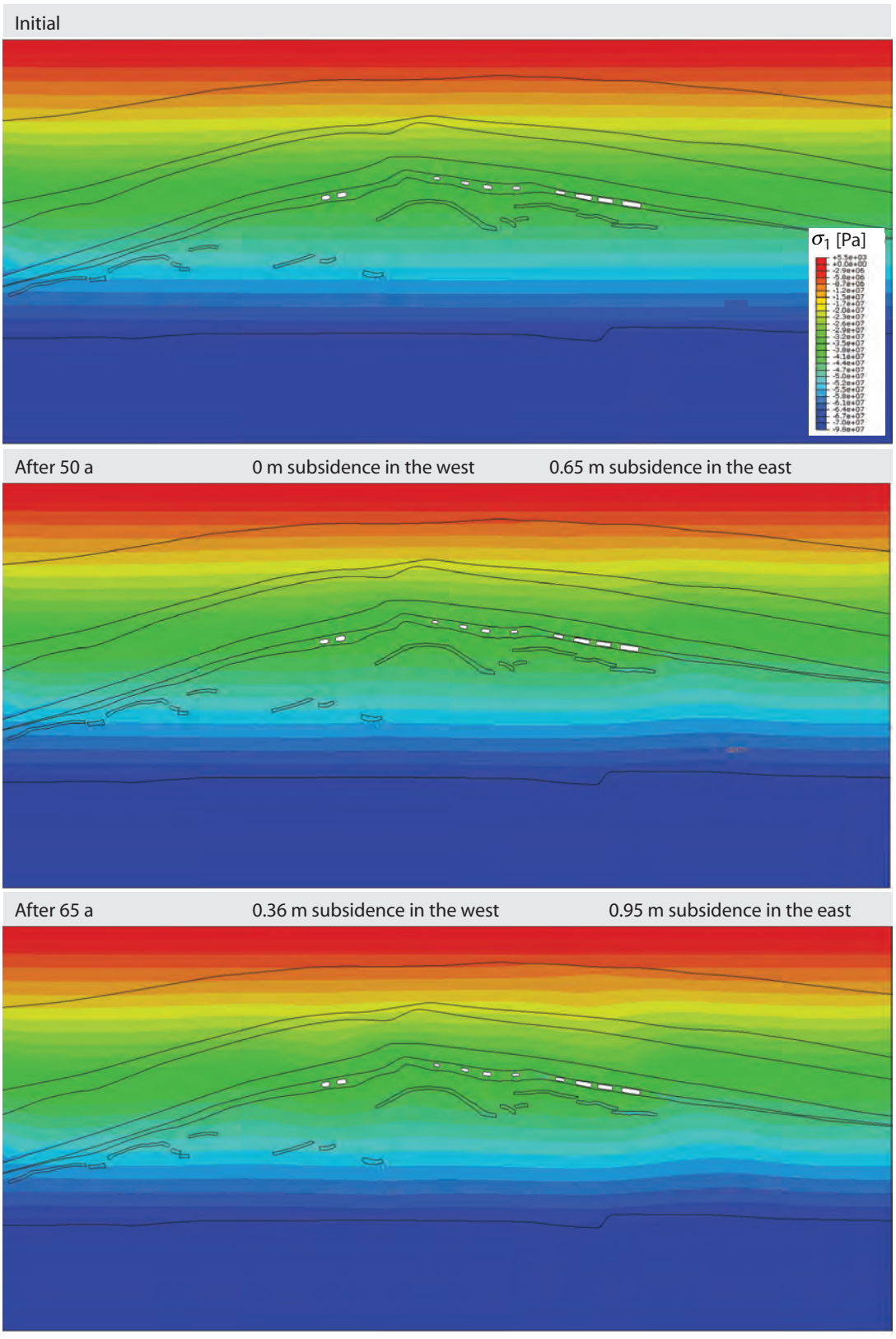

Fig. 2 - Maximum principle stress in the model, above: initial geologically stable situation, middle: after squeeze mining and subsidence in the first cavern cluster, bottom: after squeeze mining and subsidence in the first and second cavern cluster. Note that ABAQUS uses tension as positive although in subsurface studies compression is taken as positive giving the slightly confusing color bar legend.

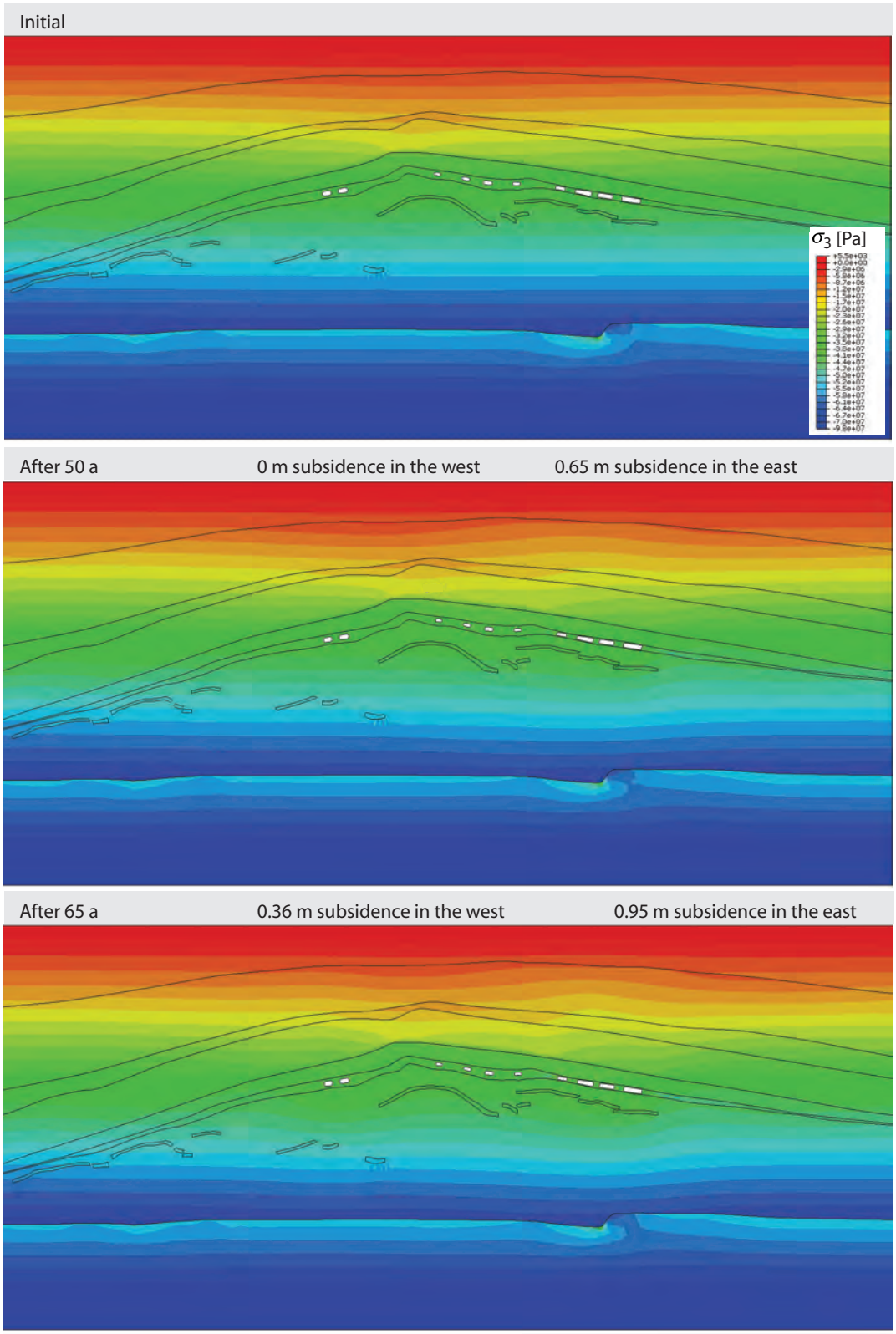

Fig. 3 - Minimum principal compressive stress in the model, above: initial geologically stable situation (note the curvature of the contours which compensates the buoyancy of the Veendam pillow), middle: after squeeze mining and subsidence in the first cavern cluster, bottom: after squeeze mining and subsidence in the first and second cavern cluster. Please note that ABAQUS uses tension as positive although in subsurface studies compression is taken as positive giving the slightly confusing color bar legend.

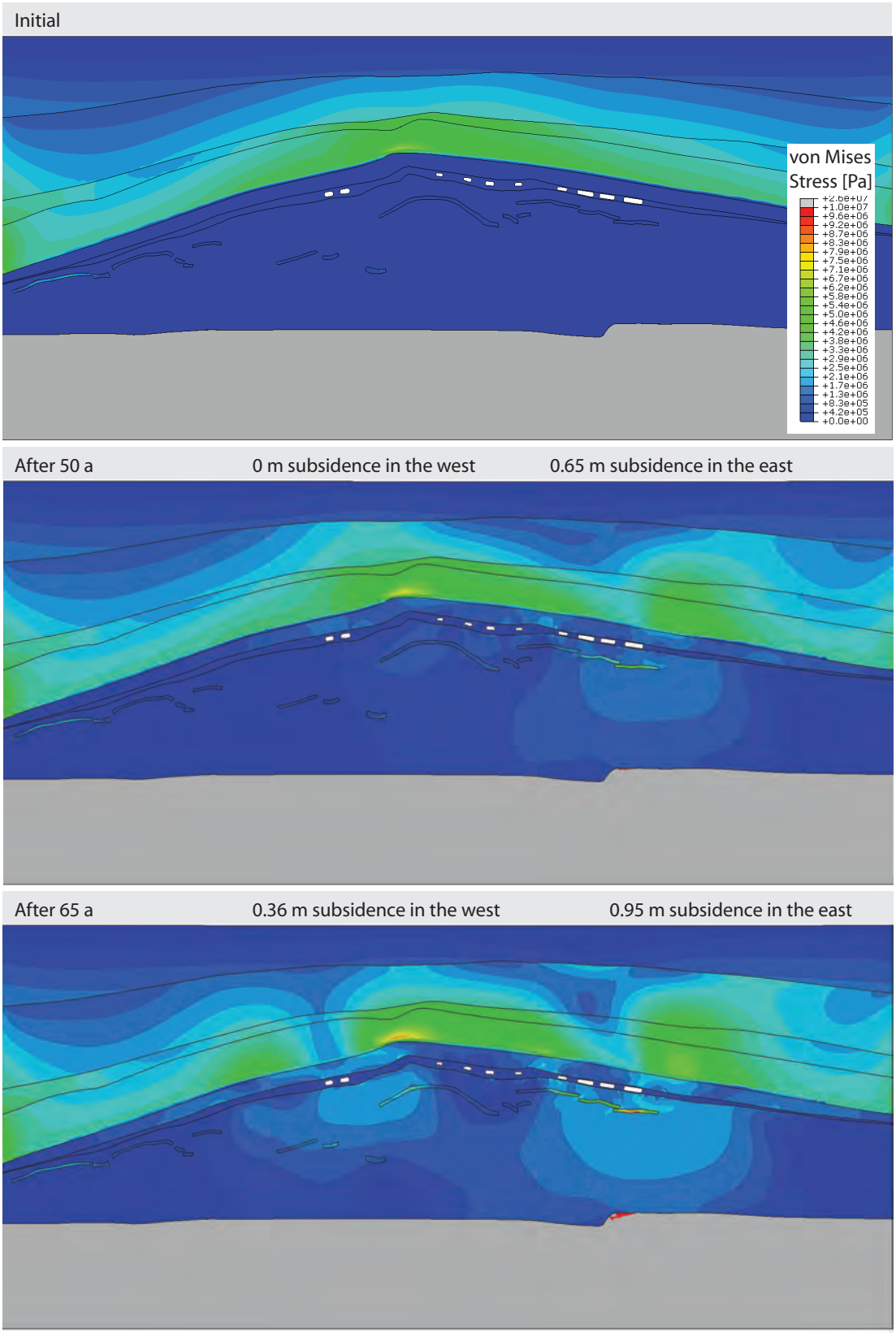

Fig. 4 – von Mises stress (shear stress) in the model, above: initial geologically stable situation (note the curvature of the contours which compensates the buoyancy of the Veendam pillow), middle: after squeeze mining and subsidence in the first cavern cluster, bottom: after squeeze mining and subsidence in the first and second cavern cluster. Note the general decrease of shear stress above the squeeze mining cavern clusters.

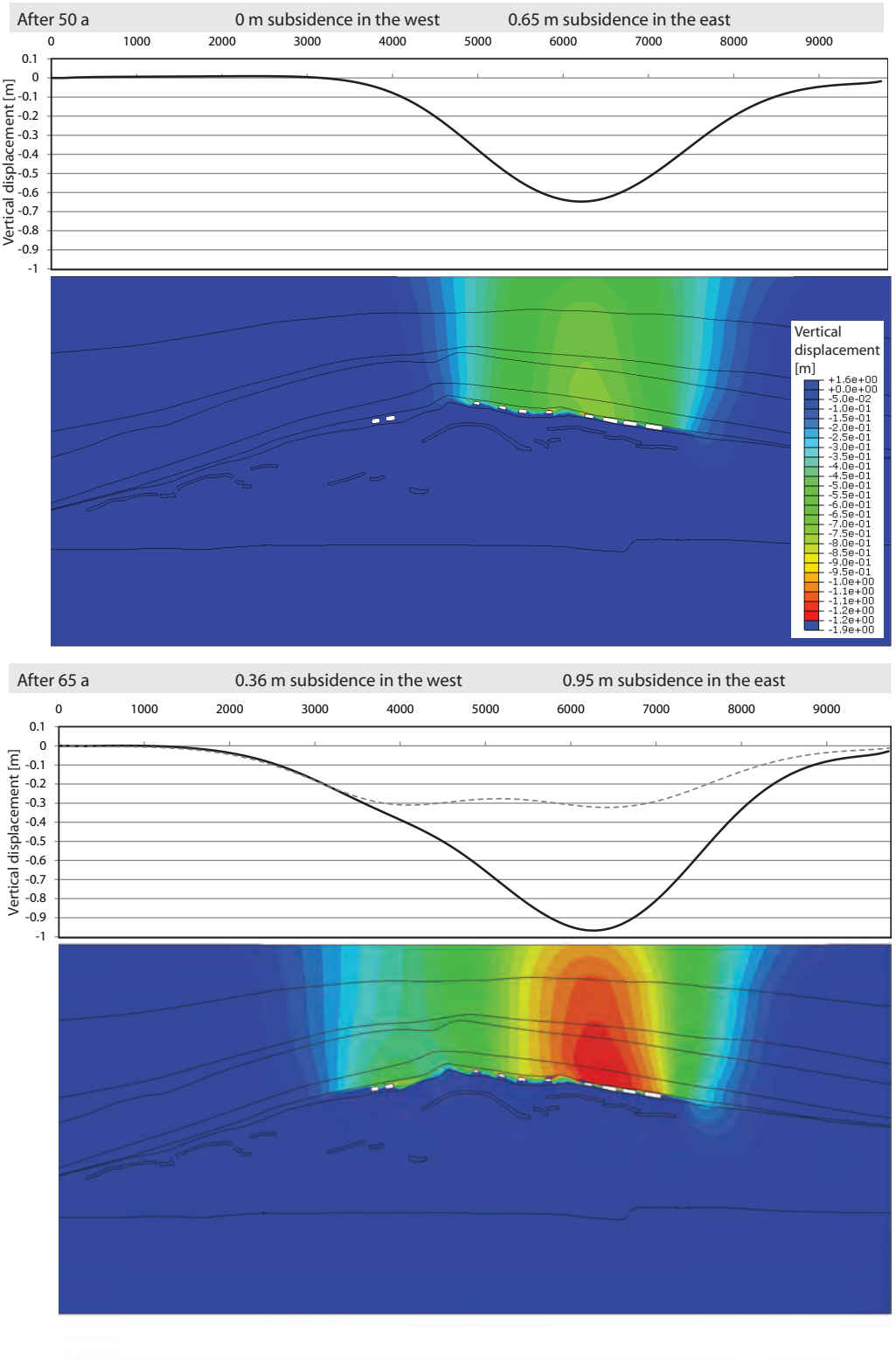

Fig. 5 – vertical displacements and surface subsidence in the model, above: after squeeze mining and subsidence in the first cavern cluster, bottom: after squeeze mining and subsidence in the first and second cavern cluster. The dashed line shows the additional subsidence (50 to 65a). Note the interplay of the two subsidence profiles in this plane strain model. Note that the lager extreme values in the color bar refer to displacements at a few nodes at the edge of the caverns.

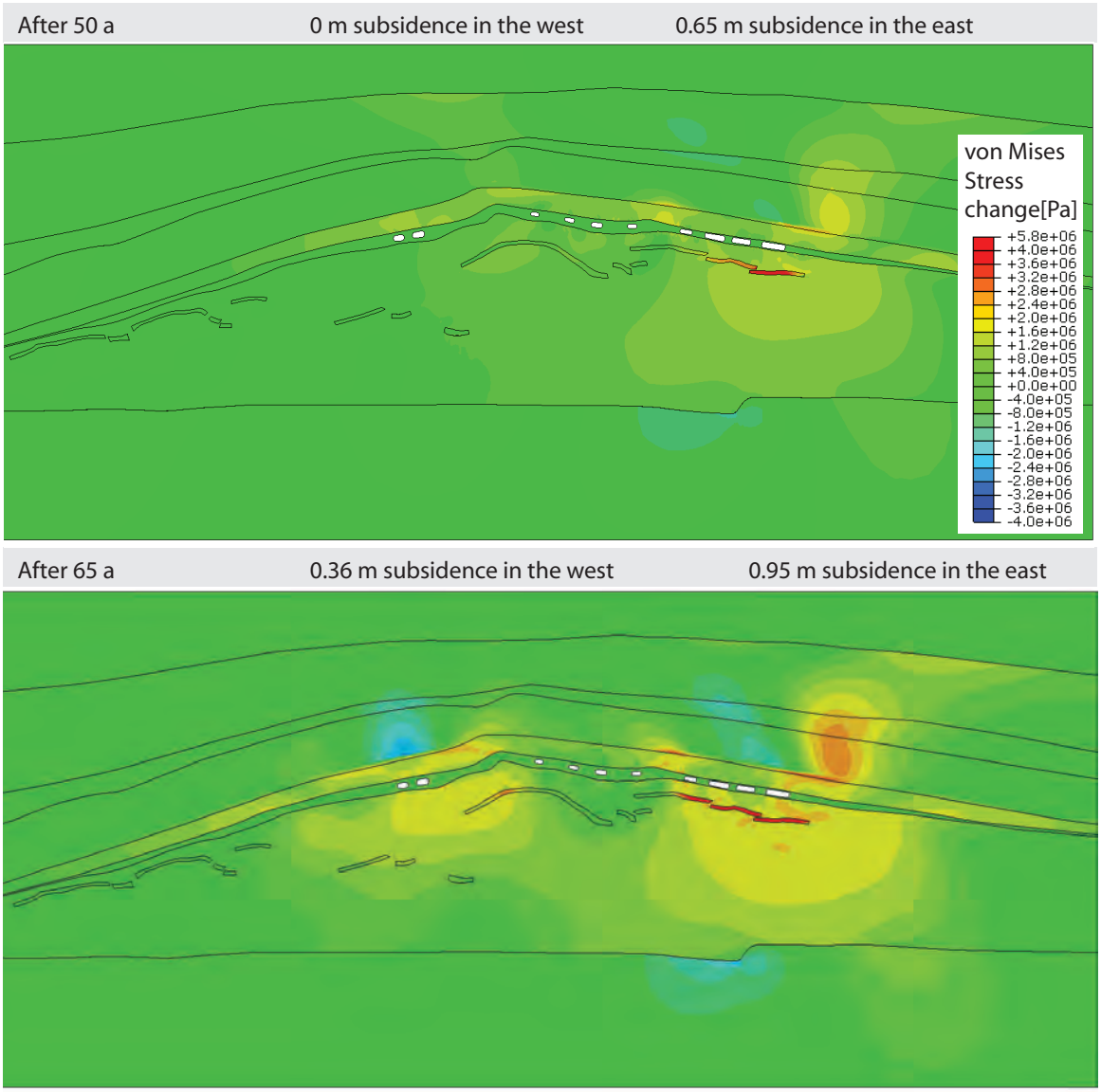

Fig. 6 – change in von Mises stress (shear stress) in the model with respect to the initial geologically stable model. Above: after squeeze mining and subsidence in the first cavern cluster, bottom: after squeeze mining and subsidence in the first and second cavern cluster. Note the general decrease of shear stress in the overburden above the squeeze mining cavern clusters.

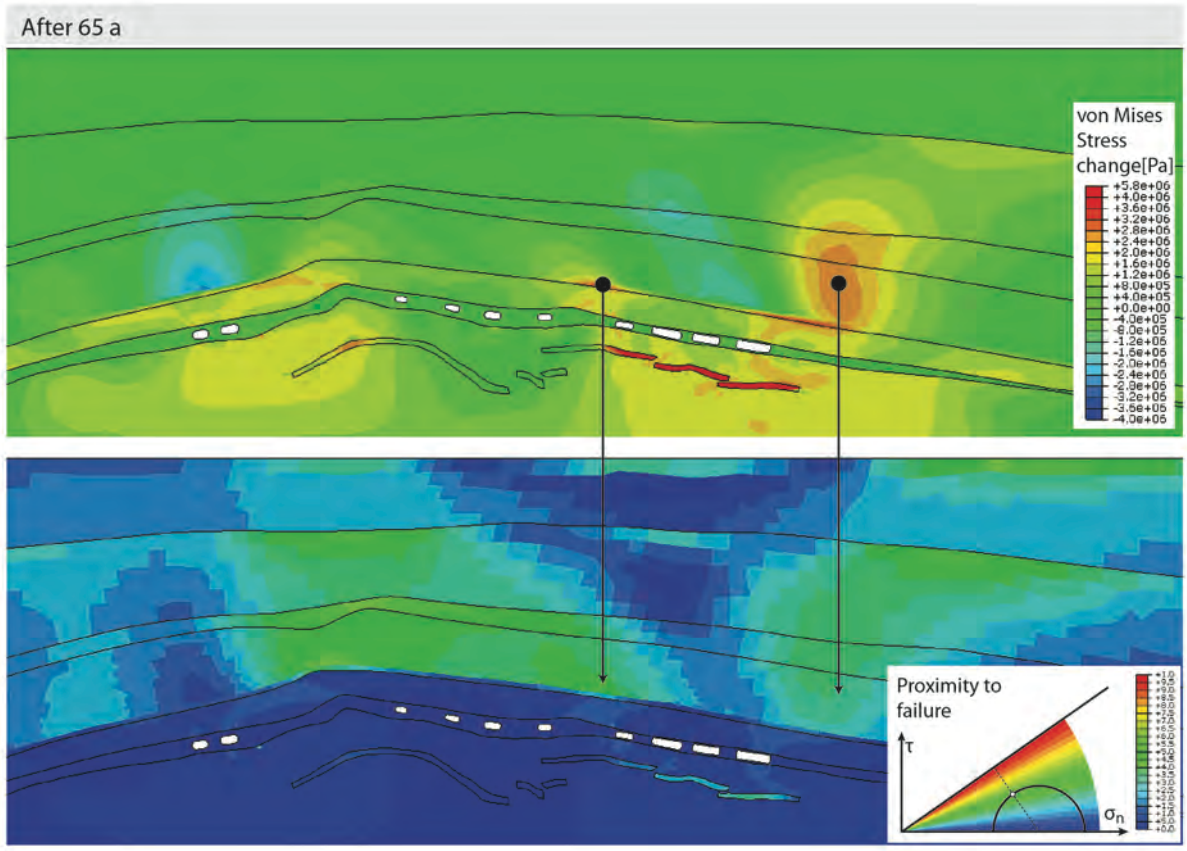

Fig. 7 – contour plot of change in von Mises stress (shear stress, same as previous figure) in the model with respect to the initial geologically stable model, final stage. Lower graph shows proximity to failure. The dots show selected locations in both diagrams.

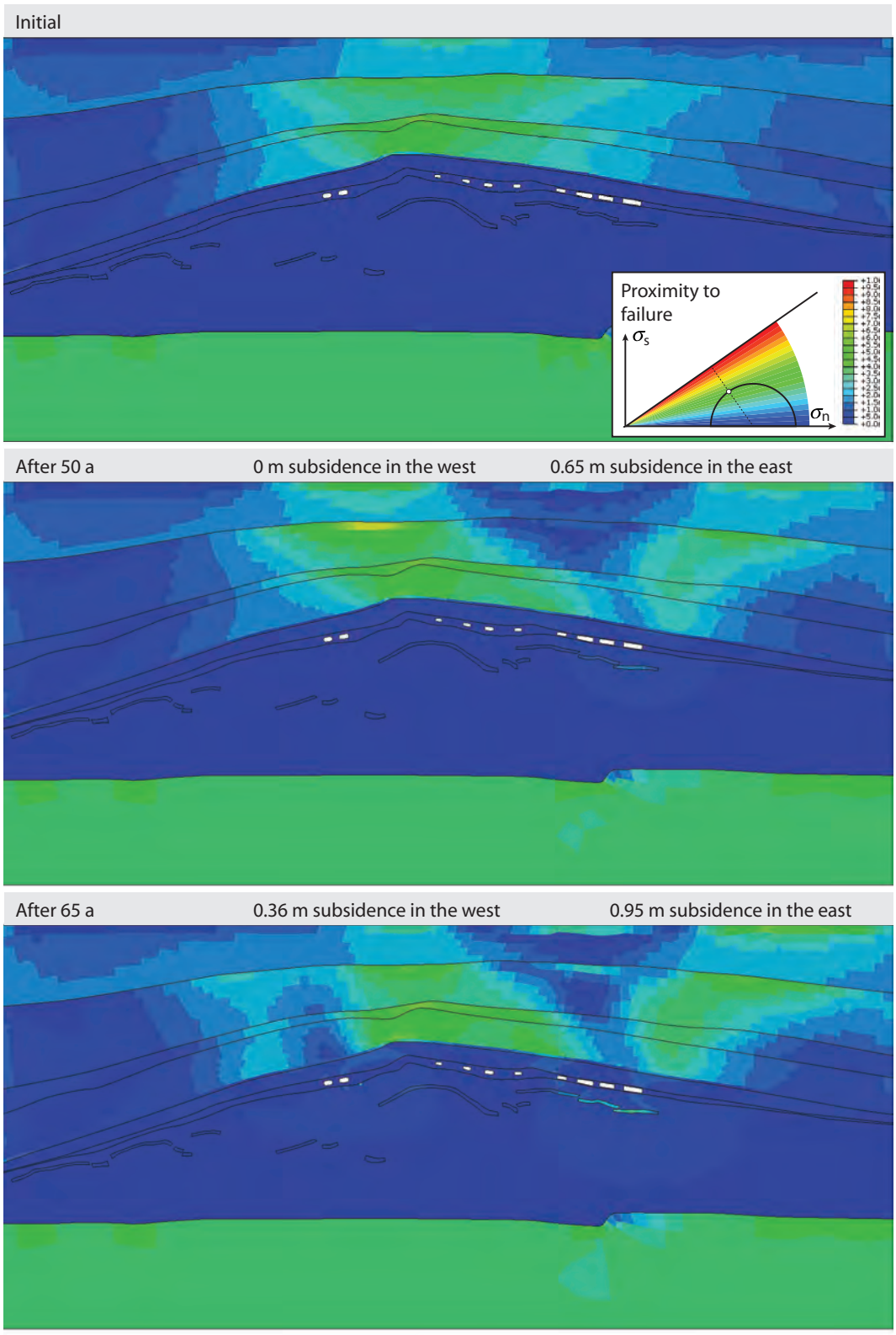

Fig. 8 – same as Fig. 7b, showing the evolution of proximity to failure.

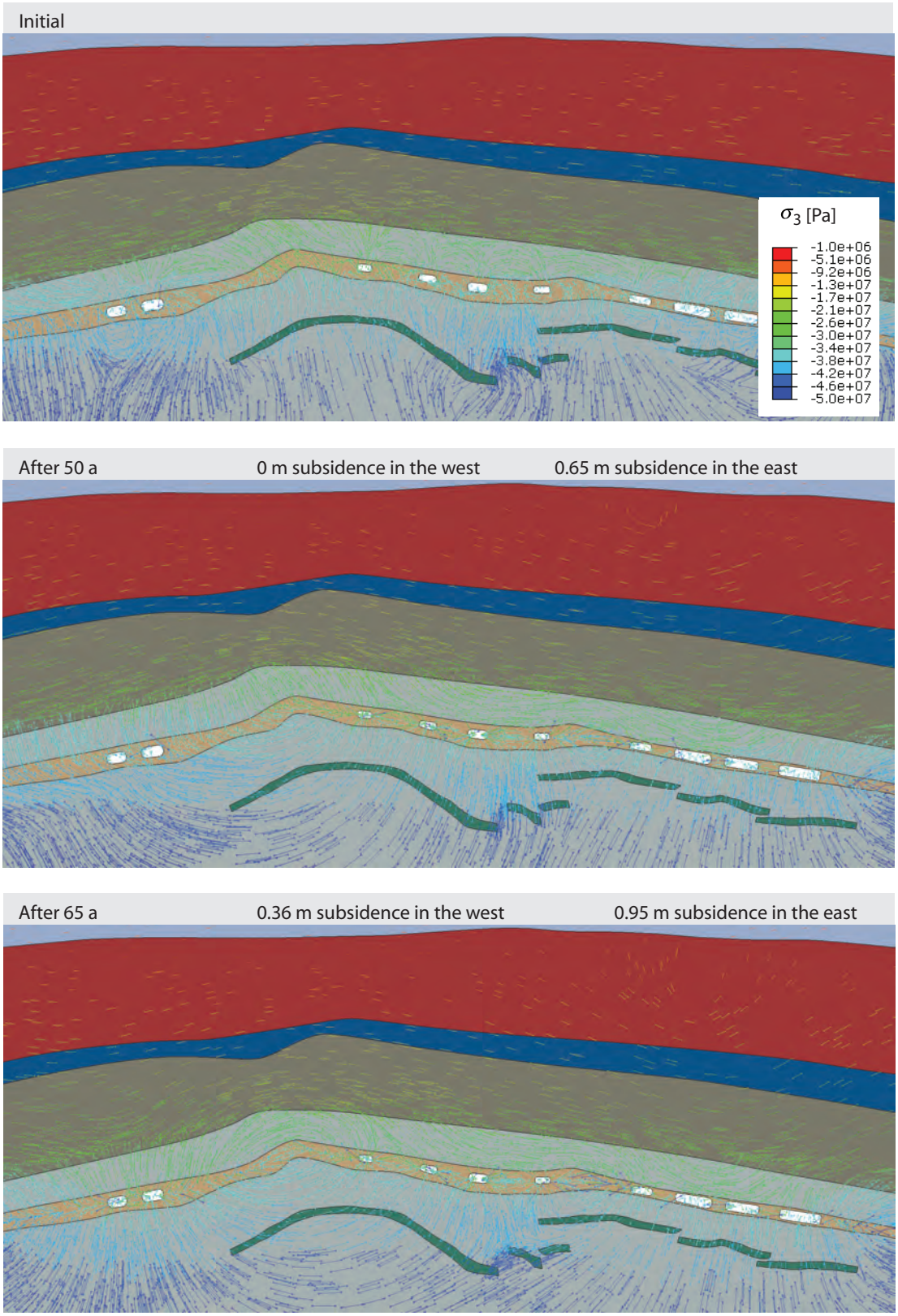

Fig. 9 – vector plots of the minimum principal stress, showing magnitude and direction in the initial model and due to squeeze mining.

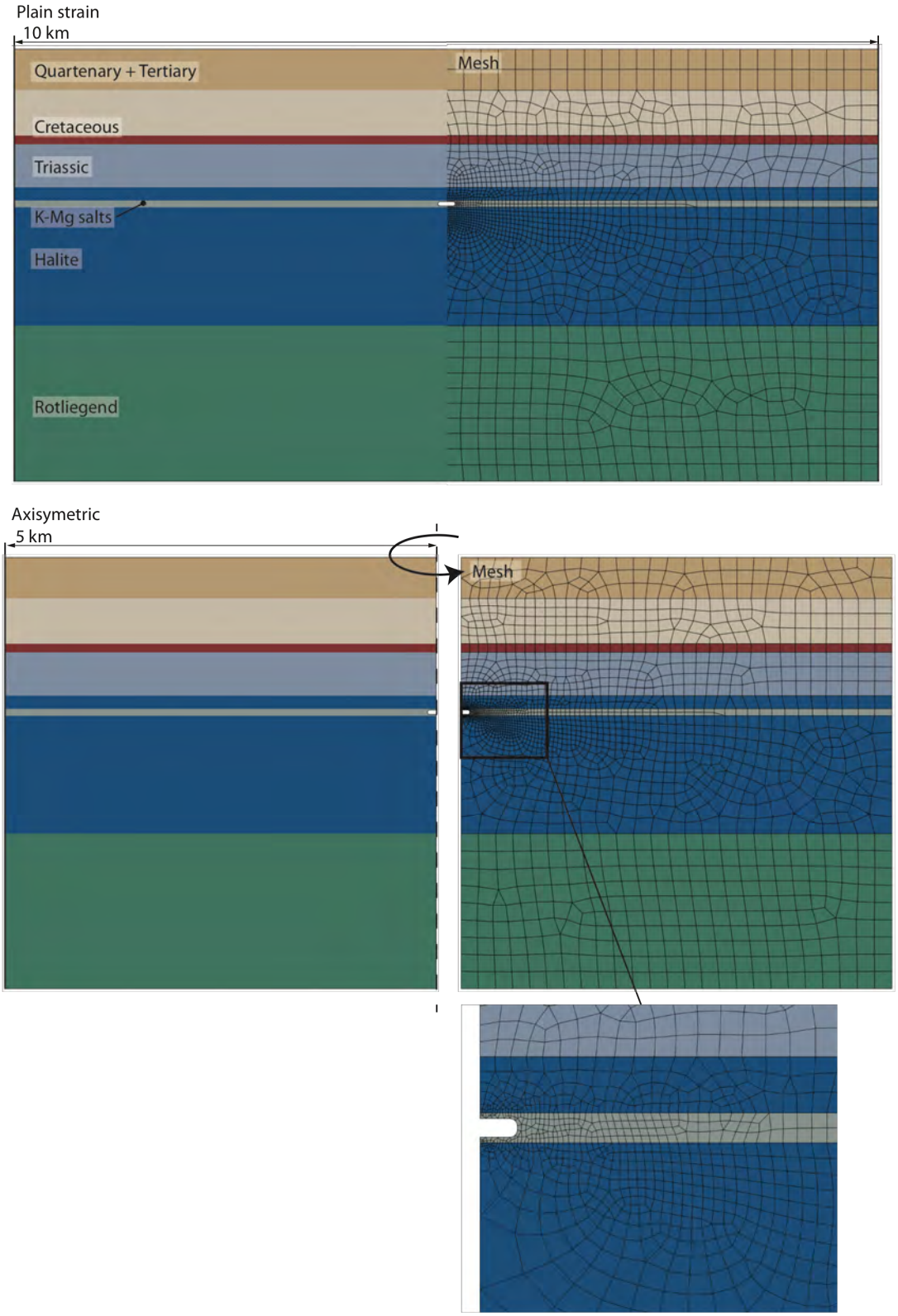

Fig. 10- The two models used to explore the difference between plane strain and axisymmetric models (single cavern), showing the finite element mesh, material groups and caverns.

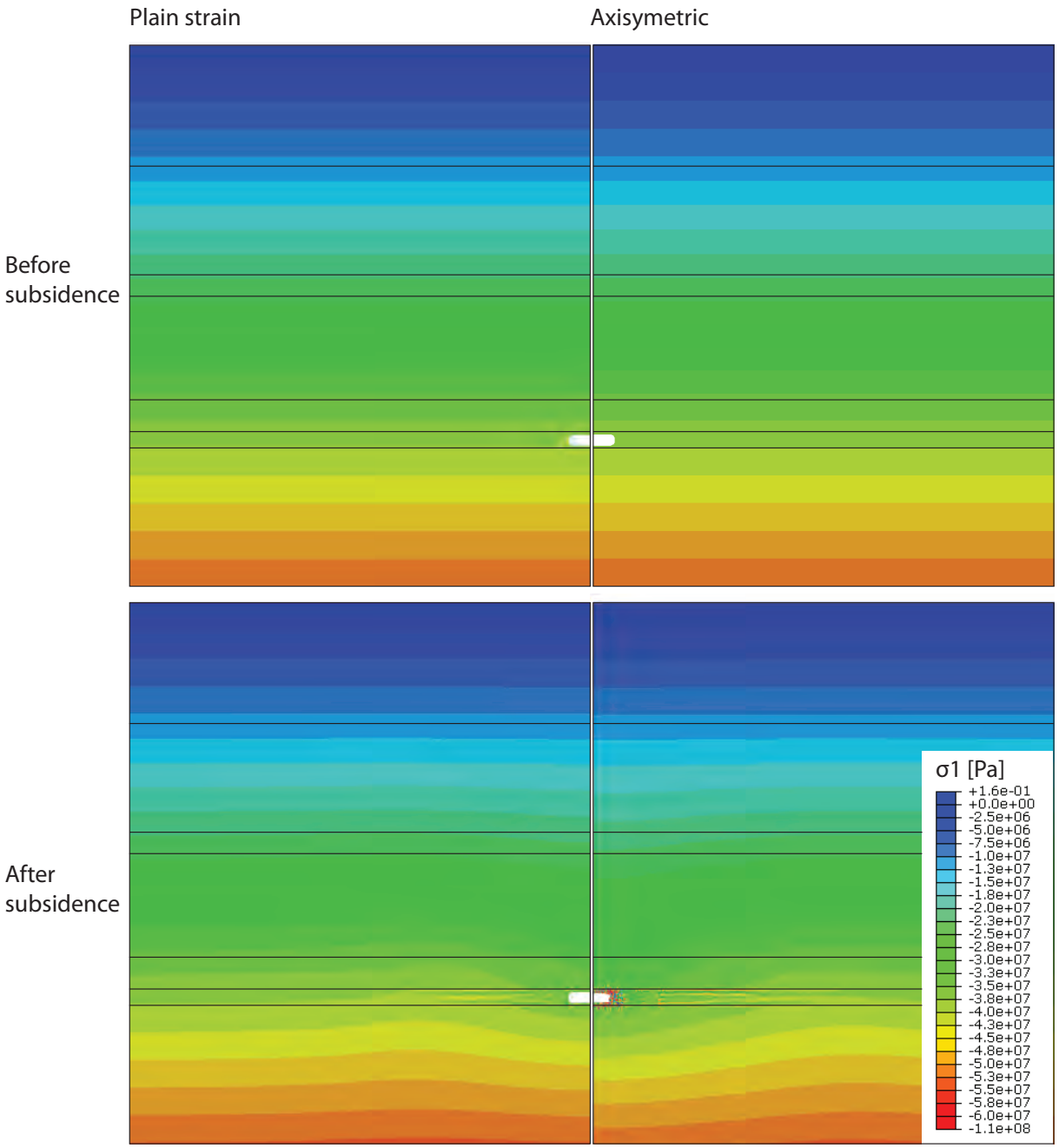

Fig. 11- comparison of the maximum principal stress between axisymmetric and plane strain models, before and after squeeze mining. Note the ABAQUS defines compressive stresses as negative.

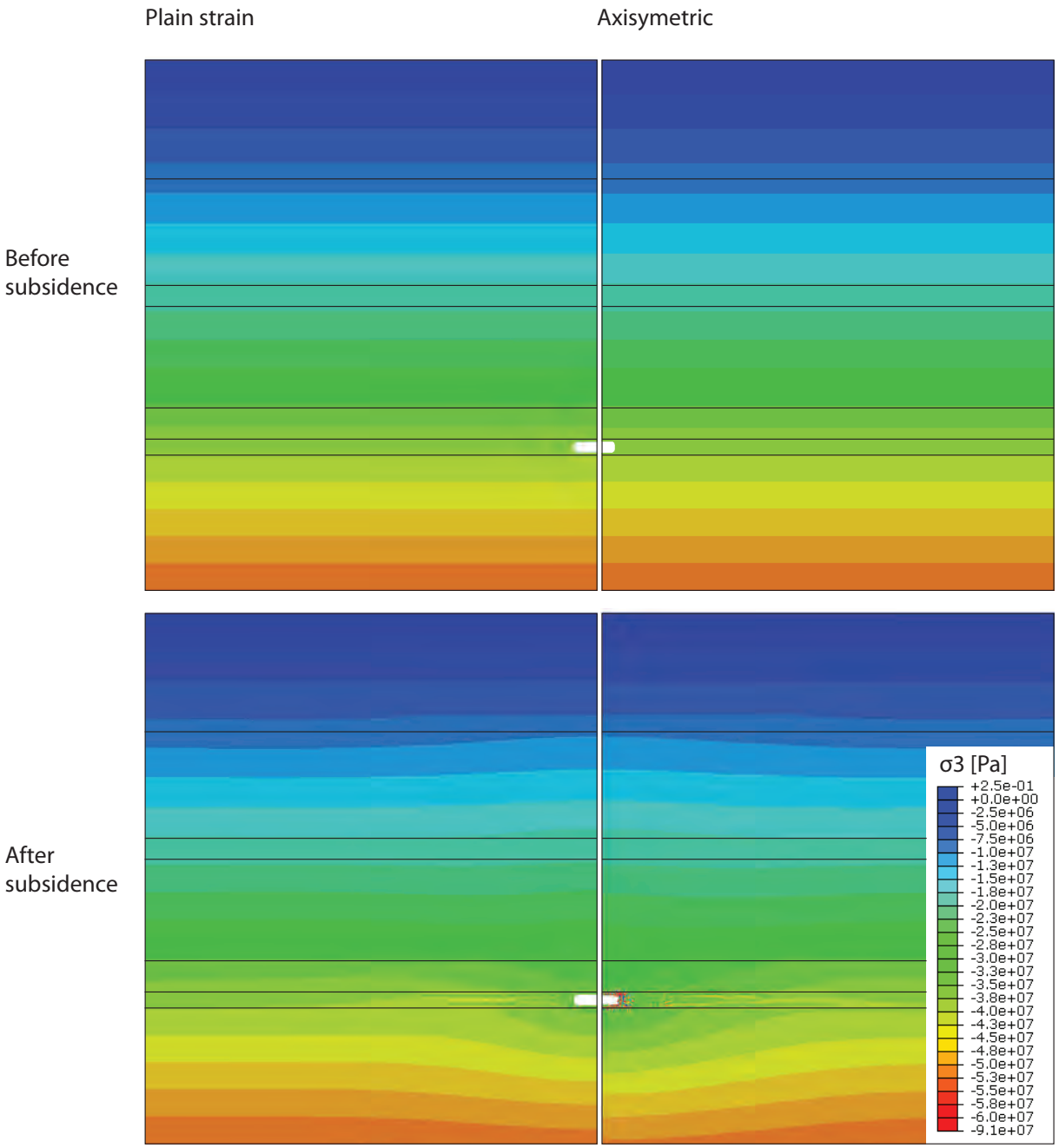

Fig. 12- comparison of the minimum principal stress between axisymmetric and plane strain models, before and after squeeze mining. Note the ABAQUS defines compressive stresses as negative.

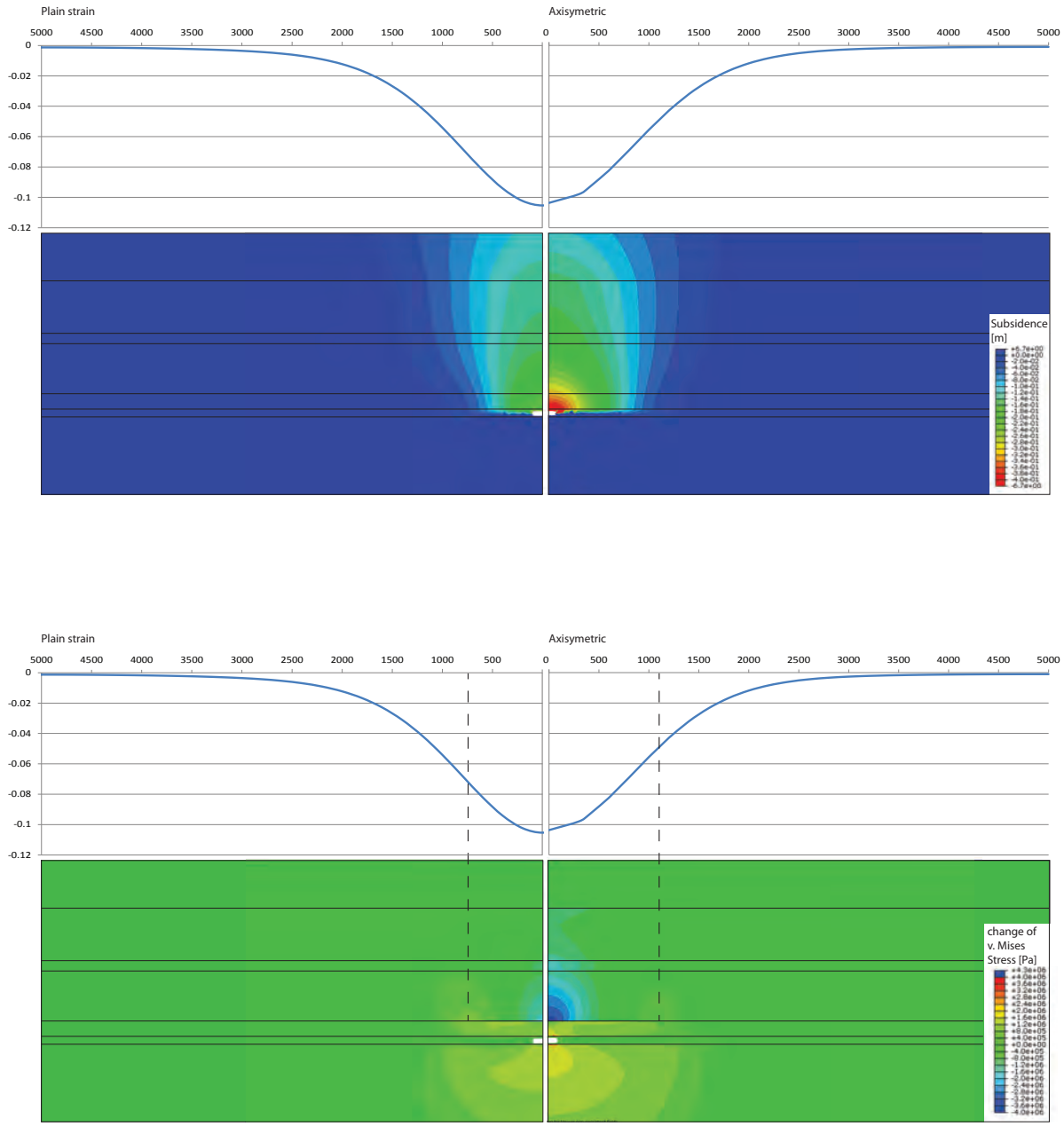

Fig. 13 - comparison of vertical displacement, subsidence profiles, and change in von Mises stress between axisymmetric and plane strain models, after squeeze mining.

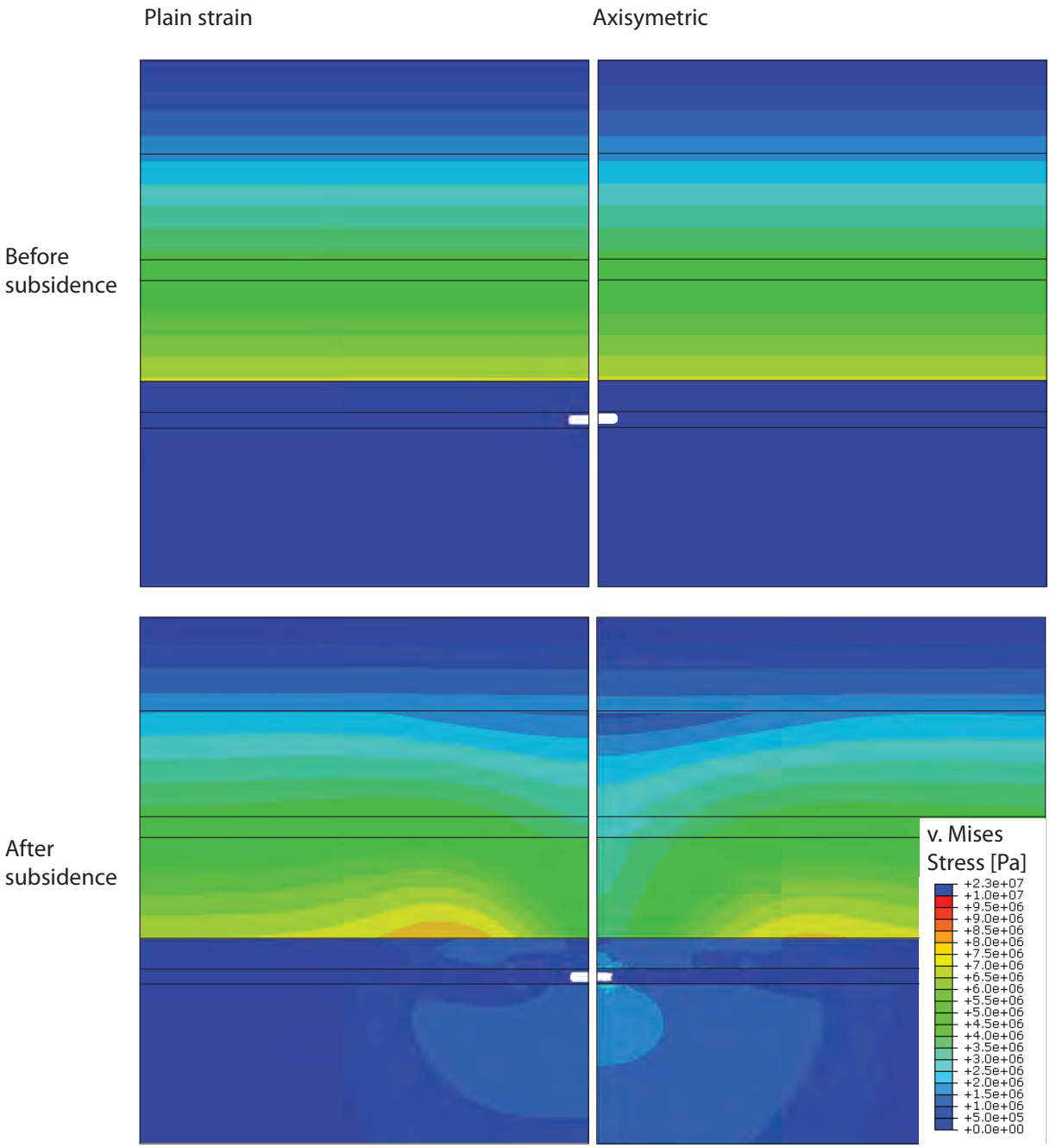

Fig. 14 - comparison of van Mises stress before and after squeeze mining between axisymmetric and plane strain models.

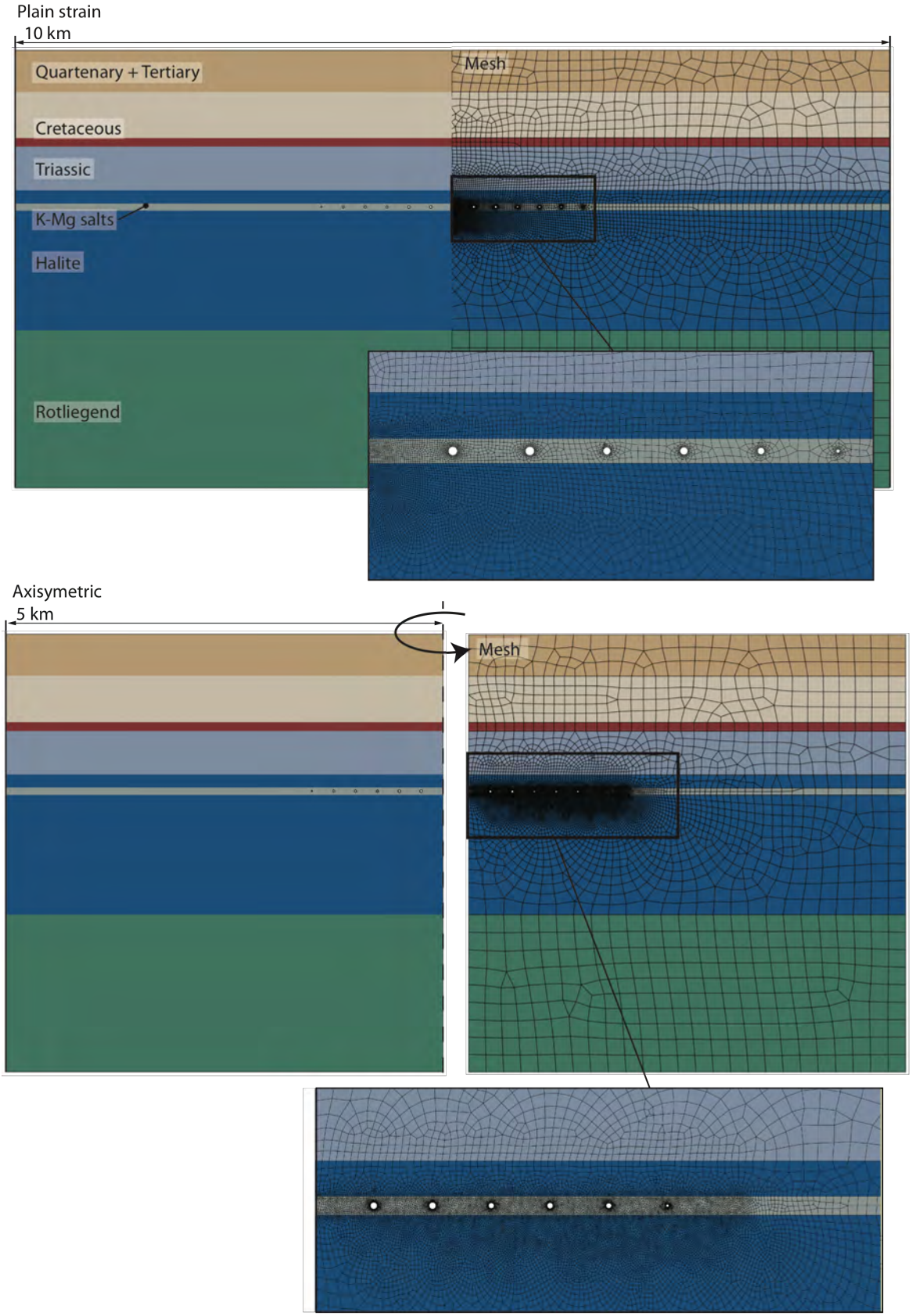

Fig. 15 - The two models used to explore the difference between plane strain and axisymmetric models (multiple caverns), showing the finite element mesh, material groups and caverns.

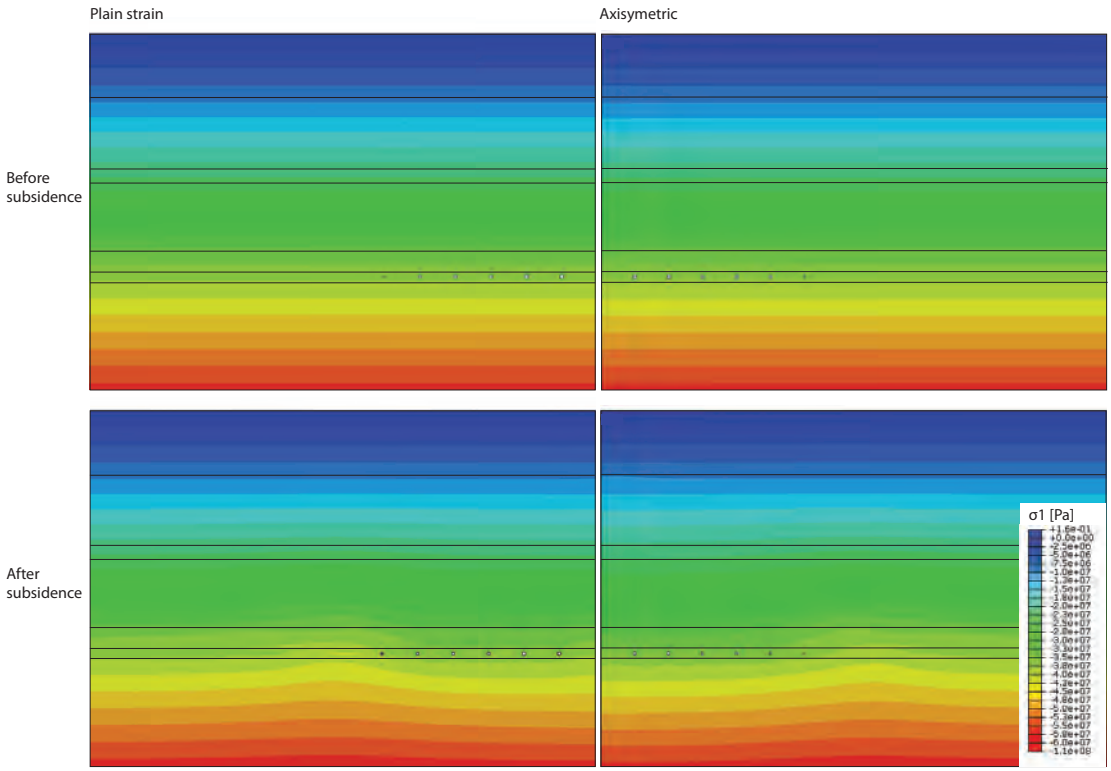

Fig. 16- comparison of the maximum principal stress between axisymmetric and plane strain models, before and after squeeze mining. Note the ABAQUS defines compressive stresses as negative.

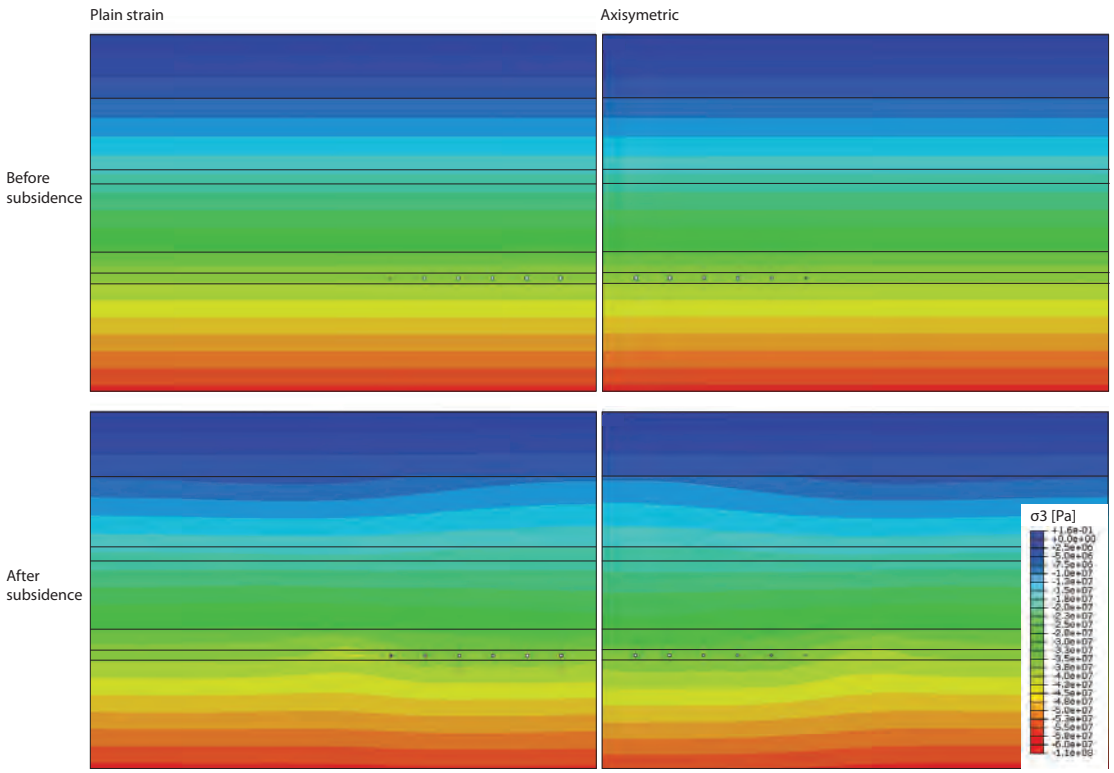

Fig. 17- comparison of the minimum principal stress between axisymmetric and plane strain models, before and after squeeze mining. Note the ABAQUS defines compressive stresses as negative.

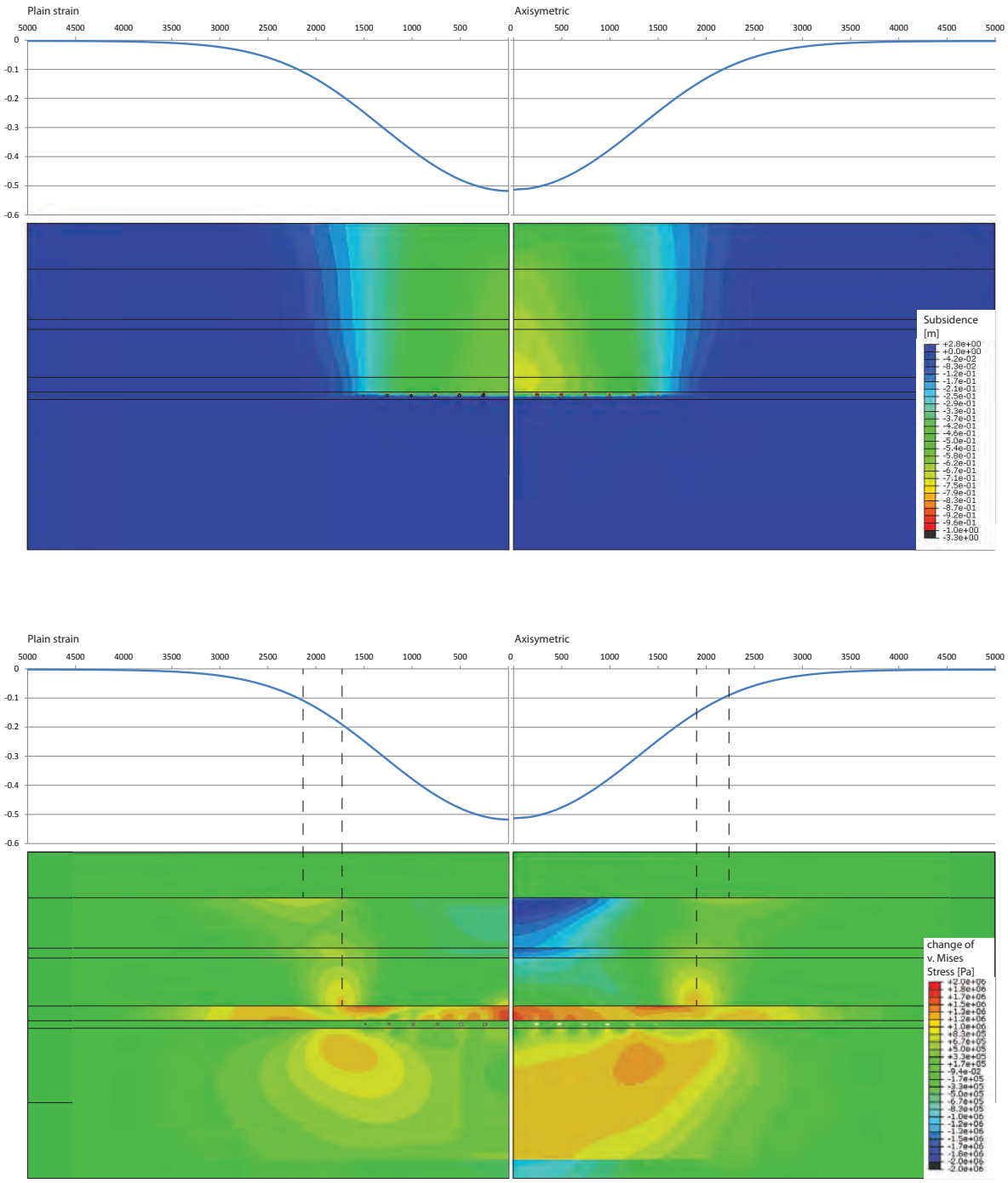

Fig. 18 - comparison of vertical displacement, subsidence profiles, and change in von Mises stress between axisymmetric and plane strain models, after squeeze mining.

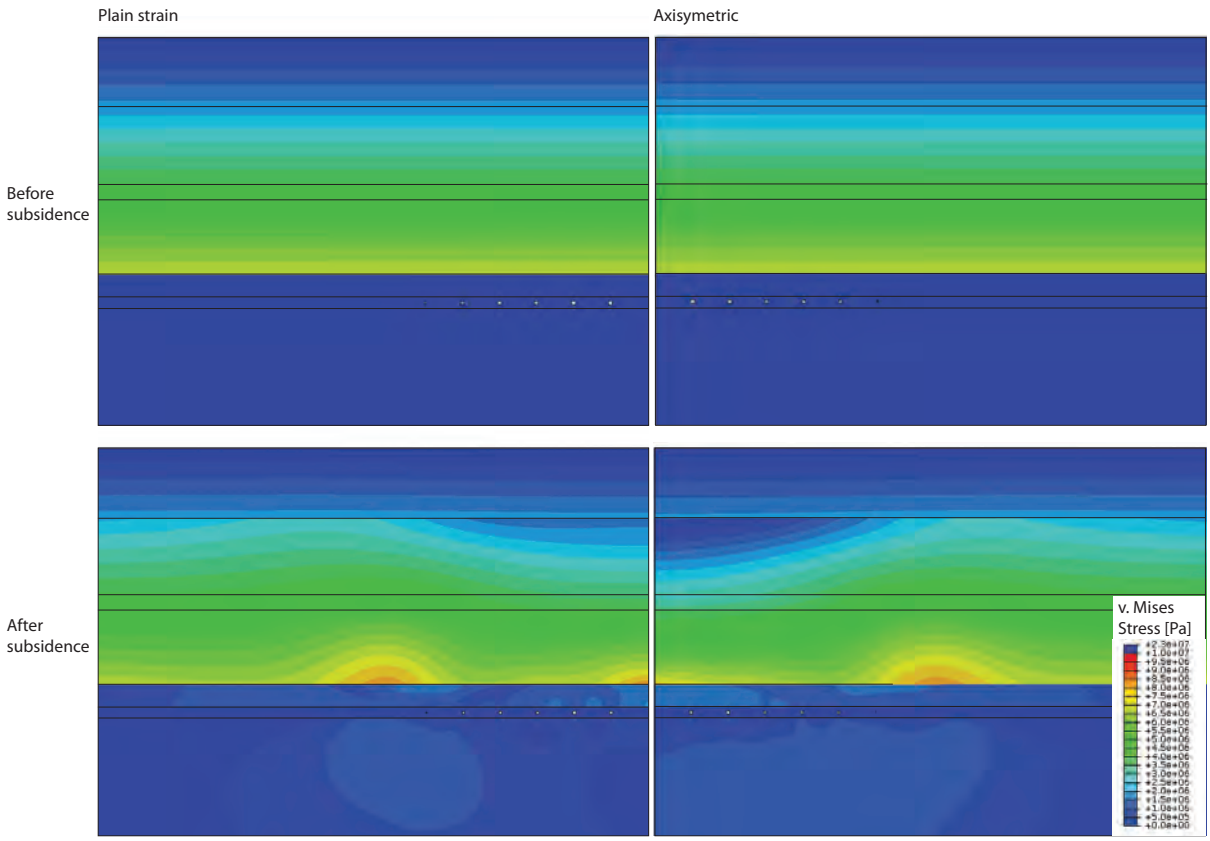

Fig. 19 - comparison of Von Mises stress before and after squeeze mining between axisymmetric and plane strain models.

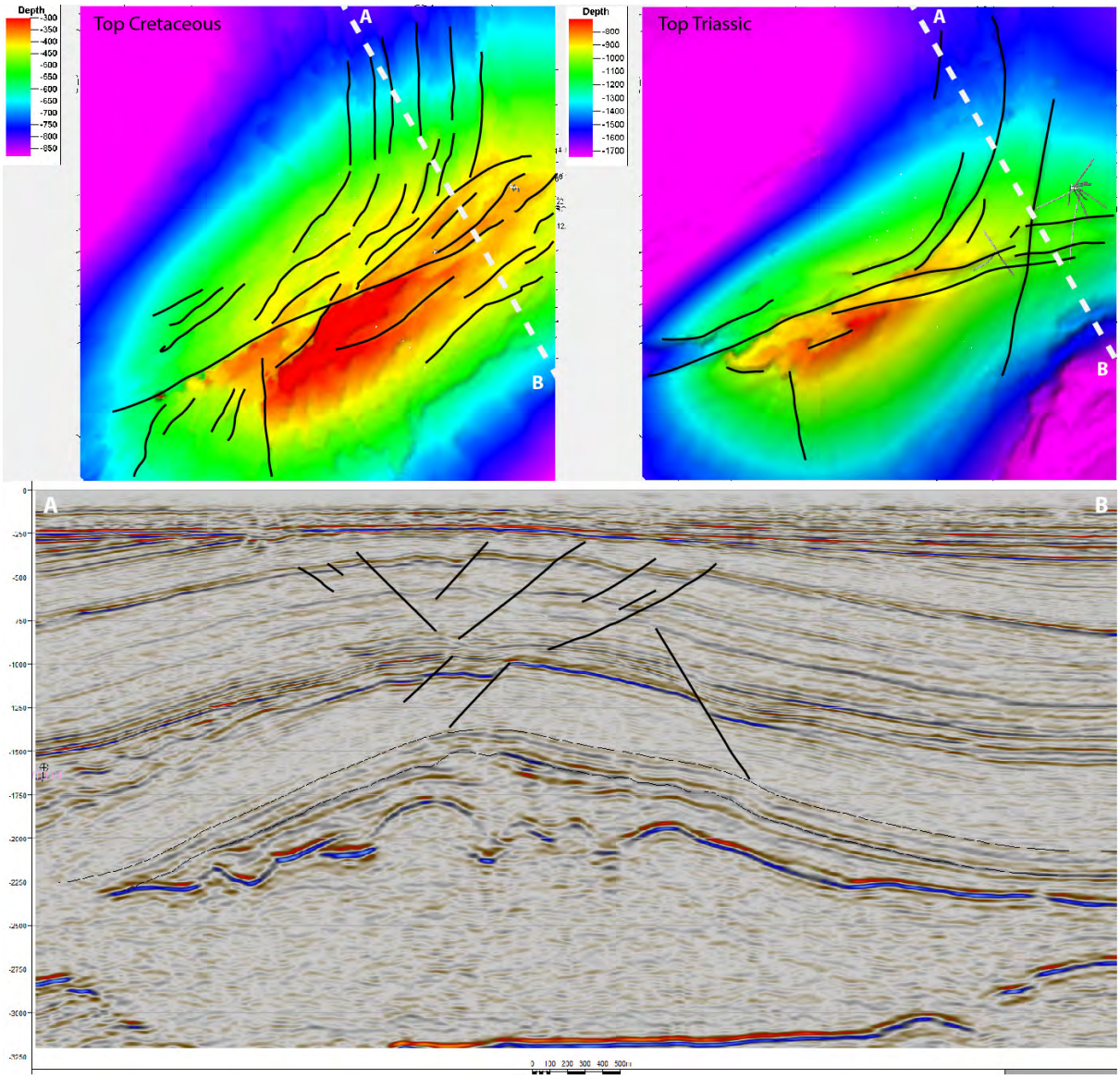

Figure 20: Top: Top Cretaceous and Top Triassic depth maps with faults indicated with black lines. Bottom: Profile A-B (vertical = horizontal scale) showing normal faults above the cavern field (from: Raith and Urai, 2017, Squeeze mining- induced stress changes in the faulted overburden of the Veendam salt Pillow, NEDMAG report).

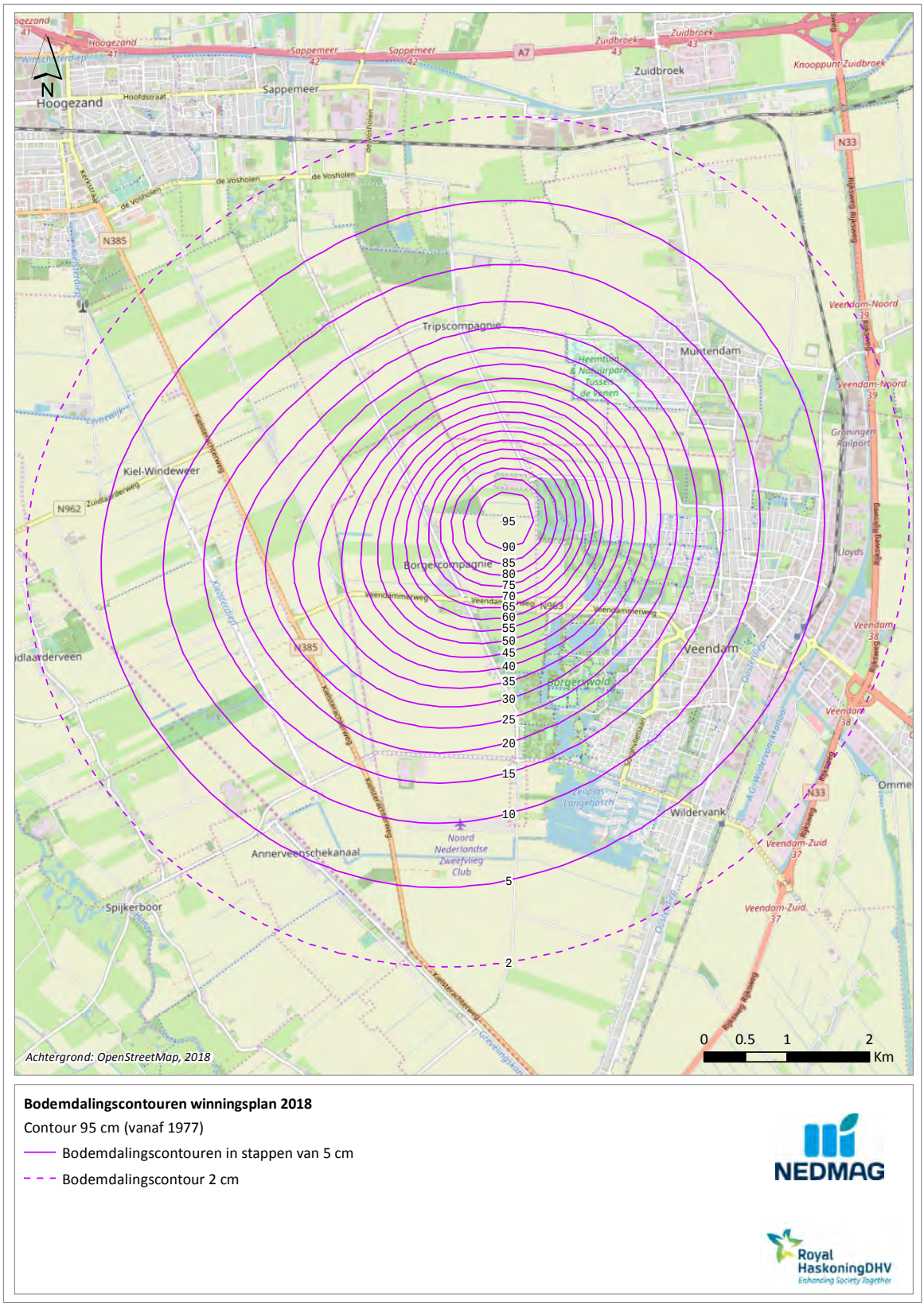

Bodemdalingscontouren winningsplan 2018

Contour 95 cm (vanaf 1977)

Bodemdalingscontouren in stappen van 5 cm

Bodemdalingscontour 2 cm

NEDMAG

Royal HaskoningDHV
Enhancing Society Together

Figure 21: Nedmag's worst case (high end) prognosis of subsidence for the Winningsplan 2018.

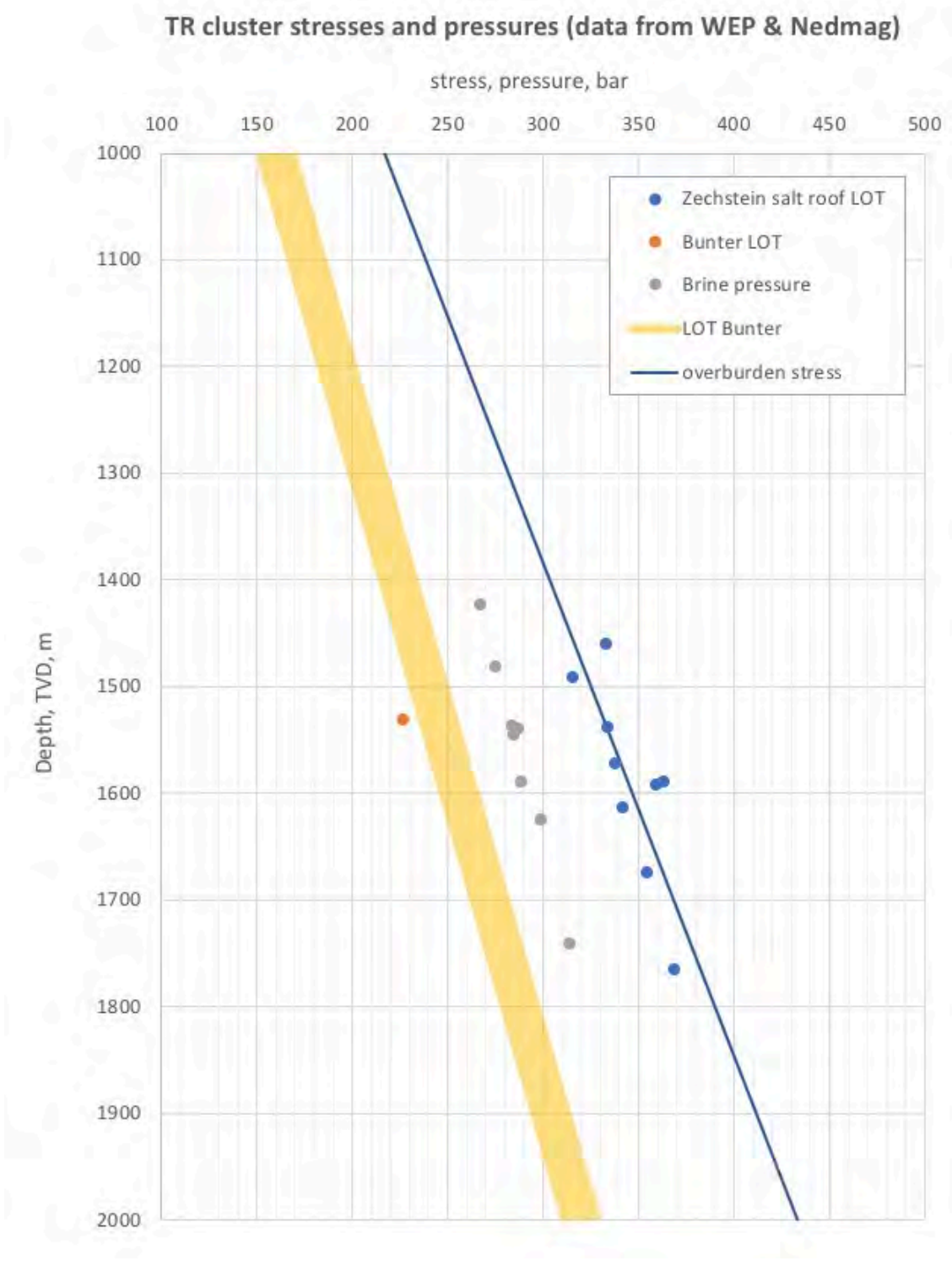

Figure 22: Plot of existing stress and pressure data from Ve and Tr wells, plus two LOT measurements (one is below the bounds of the graph) from the Buntsandstein in offset wells. The trend for Zechstein salt LOT (before the start of the mining) also illustrates the overburden trend, and the thick line for the Buntsandstein illustrates the uncertainty in the overburden stress. The cavern pressures (before the event of 20 April 2018) were about 4 MPa below the initial LOT of the Halite roof.

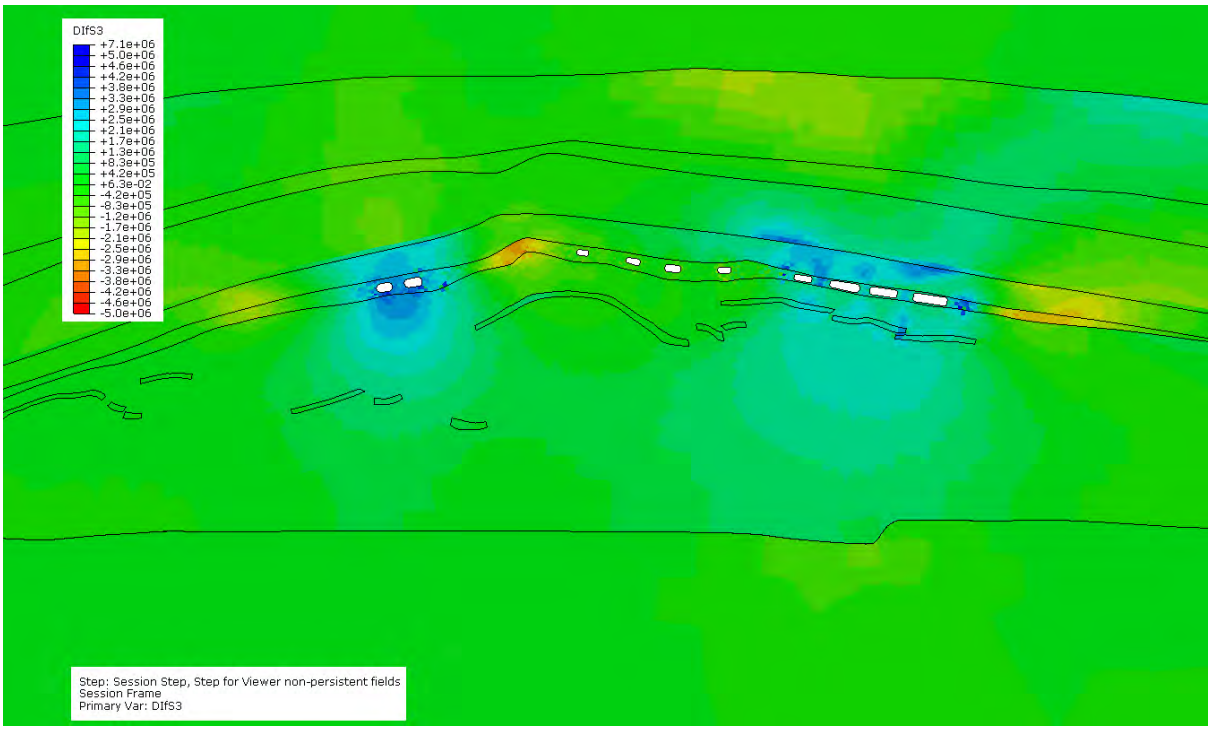

Figure 23: Changes in minimum principal stress between initial and after 65 years, focusing on the changes in the Halite roof. For the orientation of the minimum principal stress, see Fig. 9. It can be seen that the minimum principal stress above the caverns locally decreases by about 4 MPa, so that it becomes comparable to the cavern pressure (compare with Fig. 22).

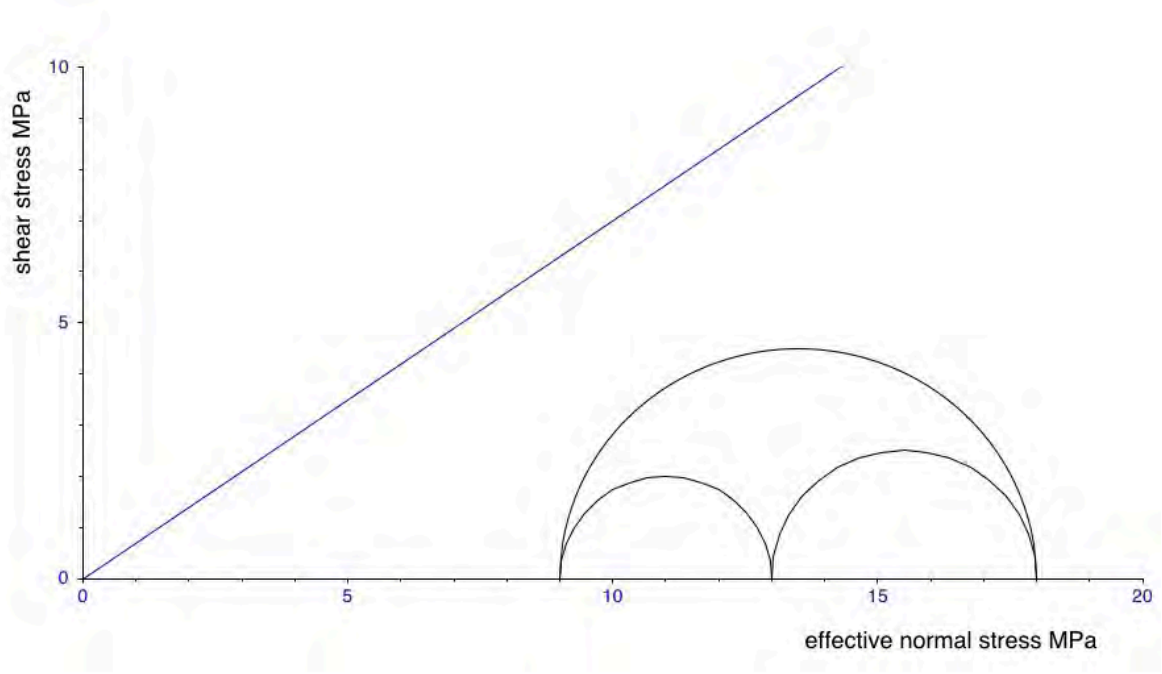

Figure 24: An illustration of the 3D effective stress state in the Buntsandstein at 1500 m depth, in the case of an intact halite roof. Values used are based on the data of Figure 3 and Figure 22 and pore pressure with SG = 1.0. For the intermediate principal stress, we assume a value about halfway between the largest and smallest principal stress.

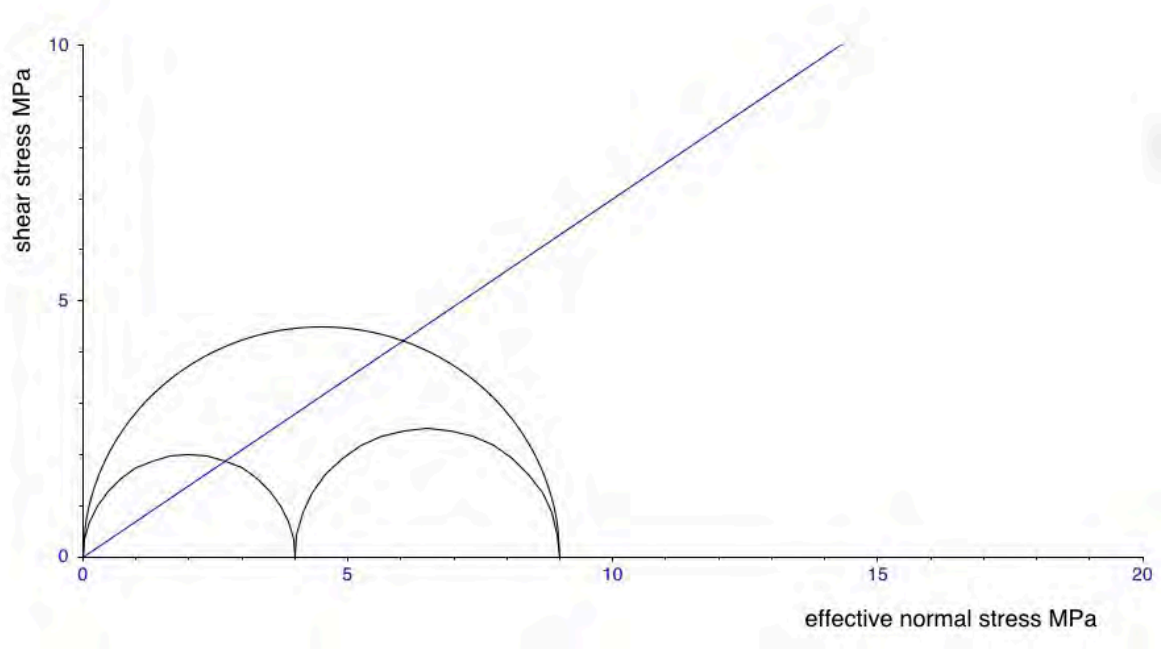

Figure 25: An illustration of the 3D effective stress state in the Buntsandstein at 1500 m depth, in the case of a leaking halite roof and corresponding increase of pore pressure to values equal to the least principal stress. Faults which are cohesionless and oriented so that they plot above the failure criterion can be reactivated.